Genetic Networks Inducing Invasive Growth in *Saccharomyces cerevisiae* Identified Through Systematic Genome-Wide Overexpression

Christian A. Shively,* Matthew J. Eckwahl,* Craig J. Dobry,* Dattatreya Mellacheruvu,† Alexey Nesvizhskii,† and Anuj Kumar*,[1]

*Department of Molecular, Cellular, and Developmental Biology and †Department of Pathology and Center for Computational Medicine and Bioinformatics, University of Michigan, Ann Arbor, Michigan 48109-1048

ABSTRACT The budding yeast *Saccharomyces cerevisiae* can respond to nutritional and environmental stress by implementing a morphogenetic program wherein cells elongate and interconnect, forming pseudohyphal filaments. This growth transition has been studied extensively as a model signaling system with similarity to processes of hyphal development that are linked with virulence in related fungal pathogens. Classic studies have identified core pseudohyphal growth signaling modules in yeast; however, the scope of regulatory networks that control yeast filamentation is broad and incompletely defined. Here, we address the genetic basis of yeast pseudohyphal growth by implementing a systematic analysis of 4909 genes for overexpression phenotypes in a filamentous strain of *S. cerevisiae*. Our results identify 551 genes conferring exaggerated invasive growth upon overexpression under normal vegetative growth conditions. This cohort includes 79 genes lacking previous phenotypic characterization. Pathway enrichment analysis of the gene set identifies networks mediating mitogen-activated protein kinase (MAPK) signaling and cell cycle progression. In particular, overexpression screening suggests that nuclear export of the osmoresponsive MAPK Hog1p may enhance pseudohyphal growth. The function of nuclear Hog1p is unclear from previous studies, but our analysis using a nuclear-depleted form of Hog1p is consistent with a role for nuclear Hog1p in repressing pseudohyphal growth. Through epistasis and deletion studies, we also identified genetic relationships with the G2 cyclin Clb2p and phenotypes in filamentation induced by S-phase arrest. In sum, this work presents a unique and informative resource toward understanding the breadth of genes and pathways that collectively constitute the molecular basis of filamentation.

THE budding yeast *Saccharomyces cerevisiae* is dimorphic, exhibiting both a unicellular growth form and a multicellular filamentous state generated presumably as a foraging mechanism under conditions of nutritional stress (Gimeno *et al.* 1992; Liu *et al.* 1993; Roberts and Fink 1994; Cook *et al.* 1996). In *S. cerevisiae*, nitrogen stress (Gimeno *et al.* 1992), growth in the presence of short-chain alcohols (Dickinson 1996; Lorenz *et al.* 2000a), and glucose stress (Cullen and Sprague 2000) can induce the transition to a filamentous form characterized morphologically as follows. Yeast cells undergoing filamentous growth are elongated in shape, due to delayed G2/M progression and prolonged apical growth (Gimeno *et al.* 1992; Kron *et al.* 1994; Ahn *et al.* 1999; Miled *et al.* 2001). Some reports indicate that these cells bud in a preferentially unipolar fashion (Gimeno *et al.* 1992; Kron *et al.* 1994), and, most distinctively during filamentous growth, daughter cells bud from mother cells but remain physically connected after septum formation (Gimeno *et al.* 1992). As a result, the interconnected cells form filaments that are termed pseudohyphae since they superficially resemble hyphae but lack the structure of a true hyphal tube with parallel-sided walls (Berman and Sudbery 2002). Depending on the induction condition and strain ploidy, pseudohyphal filaments can spread outward from a yeast colony over an agar surface and can also invade the agar (Gancedo 2001). This pseudohyphal growth response is not unique to *S. cerevisiae*; the related pathogenic fungus *Candida albicans* also exhibits pseudohyphal and hyphal morphologies, and the ability to switch between yeast, pseudohyphal,

doi: 10.1534/genetics.112.147876
Manuscript received November 21, 2012; accepted for publication February 5, 2013
Supporting information is available online at http://www.genetics.org/lookup/suppl/doi:10.1534/genetics.112.147876/-/DC1.
[1]Corresponding author: Department of Molecular, Cellular, and Developmental Biology, 830 N. University Ave., Natural Sciences Bldg., Room 4071-D, University of Michigan, Ann Arbor, MI 48109-1048. E-mail: anujk@umich.edu

and hyphal growth forms is generally considered to be necessary for virulence in *C. albicans* (Braun and Johnson 1997; Lo *et al.* 1997; Jayatilake *et al.* 2006).

Pseudohyphal growth in *S. cerevisiae* is mediated by at least three well-studied signaling pathways encompassing the mitogen-activated protein kinase (MAPK) Kss1p, the AMP-activated kinase family member Snf1p, and cyclic AMP-dependent protein kinase A (PKA). The filamentous growth MAPK cascade consists of Ste11p, Ste7p, and Kss1p (Liu *et al.* 1993; Roberts and Fink 1994; Cook *et al.* 1997; Madhani *et al.* 1997). Ste11p is a substrate of Ste20p, and Ste20p is itself regulated by the small rho-like GTPase Cdc42p and the GTP-binding protein Ras2p (Mosch *et al.* 1996; Peter *et al.* 1996; Leberer *et al.* 1997). In yeast, PKA consists of the regulatory subunit Bcy1p and one of three catalytic subunits Tpk1p, Tpk2p, or Tpk3p; Tpk2p is required for pseudohyphal growth (Robertson and Fink 1998; Pan and Heitman 1999). The adenylate cyclase Cyr1p is regulated by Ras2p (Minato *et al.* 1994); thus, Ras2p acts upstream of both the filamentous growth MAPK and PKA pathways. The serine/threonine kinase Snf1p regulates transcriptional changes associated with glucose derepression, mediates several stress responses, and is required for pseudohyphal growth (Cullen and Sprague 2000; Vyas *et al.* 2003). Snf1p, Kss1p, and Tpk2p regulate the activity of *FLO11/MUC1*, which encodes a GPI-anchored cell surface flocculin, which is a key downstream effector of pseudohyphal growth (Lo and Dranginis 1998; Rupp *et al.* 1999; Guo *et al.* 2000; Kuchin *et al.* 2002; Pan and Heitman 2002; Karunanithi *et al.* 2010).

The genetic basis of the yeast pseudohyphal growth response extends well beyond the core signaling modules outlined above (Li and Mitchell 1997; Mosch and Fink 1997; Madhani *et al.* 1999; Ma *et al.* 2007a,b; Granek and Magwene 2010; Xu *et al.* 2010). By transposon-mediated gene disruption of 3627 genes, we have previously identified 309 genes required for pseudohyphal growth in a haploid strain under conditions of butanol induction (Jin *et al.* 2008). The Boone laboratory has generated genome-wide collections of single gene deletion strains in a filamentous genetic background and has identified 700 genes required for the formation of surface-spread filaments in a diploid strain under conditions of nitrogen stress (Dowell *et al.* 2010; Ryan *et al.* 2012). Thus, loss-of-function studies identify a broad set of genes that contribute to the filamentous growth response; however, even these studies are limited in that: (1) essential genes cannot be easily analyzed other than for haploinsufficiency; (2) some deletion phenotypes may be below a threshold that can be easily observed by standard assays; and (3) many phenotypes may be obscured by compensatory buffering effects in mutational analyses that rely on single gene deletions/disruptions. Obviously, no single genetic approach can be expected to yield comprehensive results, and in this light, gene overexpression-based studies have proven to be an effective complement to loss-of-function analyses (Sopko *et al.* 2006; Douglas *et al.* 2012). Upon integration with results from the studies above, the analysis of filamentation phenotypes from gene overexpression should identify more completely the genetic scope of pseudohyphal growth.

We present here the first genome-wide overexpression analysis of yeast pseudohyphal growth. For this study, we systematically overexpressed 4909 yeast genes and identified 551 genes that enable pseudohyphal growth under conditions of normal vegetative growth. The data set was analyzed computationally to identify enriched pathways and signaling cascades, highlighting networks mediating MAPK signaling and cell cycle progression. Subsequent studies address a function for nuclear localization of the high osmolarity pathway MAPK Hog1p in repressing pseudohyphal growth, relevant to recent reports that the nuclear localization of Hog1p is not required for osmotolerance. We also identify genetic relationships with the G2 cyclin Clb2p and genes required for filamentation induced by S-phase arrest. Collectively, the work provides a valuable information resource for studies of yeast pseudohyphal growth.

Materials and Methods

Strain and growth conditions

The filamentous strains Y825, Y825/6, and HLY337 used in this study are derived from the Σ1278b genetic background (Gimeno *et al.* 1992), and all strains are listed in Supporting Information, Table S1. The genotype of haploid Y825 is *MAT***a** *ura3-52 leu2Δ0*; the genotype of diploid Y825/6 is *ura3-52/ura3-52 leu2Δ0/leu2Δ0*; and the genotype of HLY337 is *MAT*α *ura3-52 trp1-1*. Gene deletion mutants were generated using PCR-mediated gene disruption with pFA6a-kanMX6 (Longtine *et al.* 1998) or pUG72 (Gueldener *et al.* 2002). In addition to synthetic complete (SC) and SC drop-out media (US Biological), media for specific applications are described below.

The overexpression collection and high throughput plasmid transformations

The plasmids utilized for overexpression are high-copy yeast shuttle vectors, with each construct containing a yeast open reading frame (ORF) cloned under transcriptional control of a galactose-inducible promoter. The 3′ end of the open reading frame is fused in-frame with sequence encoding a triple affinity tag of His6, an HA epitope, a protease 3C cleavage site, and the IgG binding domain from protein A. In total, this plasmid collection encompasses 5854 yeast ORFs, including 4973 verified protein-coding ORFs as currently annotated in the *Saccharomyces* Genome Database (www.yeastgenome.org). It should be noted that the affinity tags may perturb protein folding at the carboxy terminus of some of the gene products, but we expect that the majority of genes in this collection (~80–90%) should encode fully functional proteins, extrapolating from large-scale protein localization and affinity purification studies (Gavin *et al.* 2002; Ho *et al.* 2002; Kumar *et al.* 2002a; Ghaemmaghami *et al.* 2003; Huh *et al.* 2003; Bharucha *et al.* 2008). To

generate overexpression strains for phenotypic analysis of filamentous growth, we introduced the plasmids individually in 96-well format into a diploid strain of the filamentous Σ1278b genetic background by a modified form of lithium acetate-mediated transformation as described (Kumar *et al.* 2000, 2002b; Ma *et al.* 2007a,b; Bharucha *et al.* 2008; Jin *et al.* 2008). All transformants were selected on SC −Ura, and glycerol stock solutions (15% glycerol) were prepared. In total, we performed 6894 plasmid preparations and yeast transformations to generate a collection of 5854 strains (~85% efficiency).

Phenotypic screening

By design of the overexpression vectors, galactose induction was used to regulate transcription of the plasmid-based target genes as follows. Yeast strains were sequentially cultured in a 30° shaking incubator in nitrogen-sufficient minimal liquid media containing glucose, raffinose, and galactose for 2–3 days, overnight, and 6 hr, respectively. Minimal liquid media consisted of 0.67% yeast nitrogen base (YNB) without amino acids and ammonium sulfate (Difco), 2% carbon source (glucose, raffinose, or galactose), 5 mM ammonium sulfate (nitrogen sufficiency), and additional amino acids to correct for auxotrophies as necessary. Following galactose induction for 6 hr, yeast cultures were spotted using a multichannel pipette onto agar plates consisting of 2% galactose, 0.67% YNB without amino acids and ammonium sulfate (Difco), 5 mM ammonium sulfate, and additional amino acids to correct for auxotrophies. Galactose induction typically drives gene expression to levels 1000-fold of those observed in the presence of glucose (St John and Davis 1981), and we estimate similar levels of inducible expression here by Western blotting (Figure S1).

The presence of galactose in the medium significantly diminished the degree of observed surface-spread filamentation for all strains, including control wild-type strains under conditions of low nitrogen, consistent with results reported in Lorenz *et al.* (2000b). Strong levels of invasive filamentation, however, were still observed, and we used this filamentation phenotype as an indicator of pseudohyphal growth. Invasive growth was assessed by a standard plate-washing assay as follows. Spotted cultures were incubated at 30° for 7 days and photographed before plate washing. Agar plates were rinsed with a gentle stream of water to remove noninvasive cells, and the remaining cells were photographed. Invasive clones were recorded and rescreened with the same protocol in a second pass. The degree of invasive growth was quantified by the pixel intensity ratio of spotted cultures pre- and postwashing.

Quantification of screen results

The level of invasiveness for each clone in the second pass was quantitatively measured using the integrated density feature of ImageJ. Images of individual clones pre- and postplate washing were analyzed after background subtraction. Scores indicate the ratios of post- to prewash pixel intensity for each indicated clone.

Plasmid construction

For galactose-independent overexpression, yeast ORFs with 1 kb upstream sequence and 300 bp downstream sequence were cloned into pRS426 (Sikorski and Hieter 1989) using standard restriction enzyme digestion and ligation techniques.

Plasmids pFA6a-GFP(S65T)-CAAX-kanMX6 and pFA6a-GFP(S65T)-CAAX-HIS3MX6 carrying GFP-CAAX modules were modified from pFA6a-GFP(S65T)-kanMX6 and pFA6a-GFP(S65T)-HIS3MX6 (Longtine *et al.* 1998). The *Pac*1 and *Asc*1 restriction sites of these plasmids were used to replace the GFP module with a GFP-CAAX module, generated by PCR amplification using a 3′ primer encoding the nine carboxy-terminal residues of the budding yeast Ras2p CAAX box (Westfall *et al.* 2008). The following forward and reverse primers were used: HOG1_RAS_F1: CGGTAACCAGGCCATA CAGTACGCTAATGAGTTCCAACAGCGGATCCCCGGGTTAAT TAA and HOG1_RAS_R1: TCTTTTTTTTTTTGTTTCCTCTA TACAACTATATAC GTAAGAATTCGAGCTCGTTTAAAC. All plasmids are available upon request.

Galactose-independent overexpression

Y825/6 strains with overexpression vectors (pRS426 carrying yeast ORFs with 1 kb upstream sequence and 300 bp downstream sequence) were streaked on synthetic low ammonium dextrose (SLAD) plates (2% glucose, 0.67% YNB without amino acids and ammonium sulfate, 50 μM ammonium sulfate, and supplemental leucine to correct for auxotrophy). Plates were incubated 5 days at 30° prior to imaging.

Verification of overexpression by Western blotting

Selected moveable open reading frame (MORF) strains of the Y825/6 background were cultured in 5 ml SC −Ura media overnight at 30°, followed by back dilution into nitrogen sufficient minimal media with galactose for 4 hr. Following protein extraction, SDS–PAGE resolution and transfer to nitrocellulose membrane by standard procedures, membranes were incubated with protein A antibody against the tandem affinity purification (TAP) tag in a 1:10,000 dilution. Blots were developed using SuperSignal West Dura Extended Duration Substrate (Thermo Scientific).

Identifying network modules and signaling cascades by computational analysis

The gene set identified from this overexpression screen was submitted to the functional analysis tool DAVID (Huang Da *et al.* 2009) to identify enriched Kyoto Encyclopedia of Genes and Genomes (KEGG)-annotated pathways. Since the overexpression screen was genome-wide in scope, the default background set was used. The most enriched pathways, mediating cell cycle progression (sce04111), meiosis (sce04113), and MAPK signaling (sce04011), were selected for further analysis. The KEGG.xml files of these pathway maps were downloaded and parsed using an in-house program that generates nodes and edge lists. The KGML pathway .xml (kgml) file consists of "entry" tags, which can be represented as nodes, and "relation" tags, which can be represented as edges of

a network. The entry tags consist of genes, compounds, and complexes, while the relation tags include manually curated molecular interactions, reaction networks, genetic and environmental information processing, and cellular networks (Kanehisa *et al.* 2012). Cytoscape (Killcoyne *et al.* 2009), which constructs a ball-and-stick representation of a network using an edge list, was used to visualize the network. Since the three pathways possess overlapping gene sets, the edge lists were concatenated and visualized as one single network.

Cell cycle analysis

For *CLB2* epistasis analysis, a sampling of 10 genes was selected that fulfilled the following criteria: (1) genes that had been identified in this overexpression screen as yielding filamentous growth under noninducing conditions of nutrient sufficiency; and (2) genes that had either not been placed in a clear signaling pathway or that functioned in a pathway with unclear upstream components. The sampled gene set was not intended to be comprehensive, but rather served as a probe for additional genes that may contribute to filamentation through mechanisms that impact *CLB2* and cell cycle progression. Homozygous diploid double deletion mutants were constructed for this analysis, and the mutant strains were streaked onto SC agar plates, incubated overnight at 30°, and then photographed. For surface-spread filamentation using hydroxyurea treatment, hydroxyurea was added to SC agar plates to a final concentration of 100 mM (Kang and Jiang 2005). Strains were photographed following overnight incubation at 30°.

Invasive growth analysis of strains with modified HOG1 alleles

Yeast strains of the Y825 genetic background containing integrated *HOG1-GFP*, *HOG1-GFP-CAAX*, and *hog1*Δ alleles were assayed for invasive growth by plating spotted cultures on SLAD plates (2% glucose, 0.67% YNB without amino acids and ammonium sulfate, 50 μM ammonium sulfate, and supplemental amino acids to correct for auxotrophies) with 1% (vol/vol) butanol. Plates were sealed in parafilm and incubated for 7 days at 30°. Strains were assayed for invasive growth by rinsing with water and rubbing away nonadherent cells (Cullen and Sprague 2000). Spotted cultures were photographed pre- and postwash, and invasiveness was measured using the integrated density feature of ImageJ.

β-Galactosidase assays

The *FRE-lacZ* reporter construct (Madhani and Fink 1997) was used to measure filamentous growth signaling using the Yeast β-Galactosidase Assay kit (Thermo Scientific) according to protocols described previously (Ma *et al.* 2008; Xu *et al.* 2010).

Fluorescence microscopy

Fluorescence images were taken using a DeltaVision-RT Live Cell Imaging system (Applied Precision). Image capture was conducted using Applied Precision's SoftWorx imaging software.

Results

Generating a mutant collection for genome-wide overexpression analysis

Standard laboratory strains of *S. cerevisiae* (*e.g.*, derivatives of S288c) are nonfilamentous and, consequently, inappropriate for studies of pseudohyphal growth. The Σ1278b strain has emerged as the preferred background for studies of filamentation, since it undergoes a significant and easily controlled transition to filamentous growth (Grenson 1966; Gimeno *et al.* 1992); however, no genome-wide mutant collections suitable for this study have been generated previously in the Σ1278b background (Coelho *et al.* 2000). Here, we sought to construct an extensive reagent base for overexpression studies of pseudohyphal growth, generating a collection of yeast strains in Σ1278b with each mutant carrying a single plasmid enabling galactose-inducible gene overexpression. For this purpose, we utilized the plasmid collection constructed in Gelperin *et al.* (2005) and introduced the plasmids individually by transformation into diploid yeast. Of the 5854 plasmids encompassed in this overexpression collection, we identified 4909 clones that: (1) contained an ORF corresponding to an annotated and verified yeast gene and (2) allowed for sufficient cell growth upon galactose induction in the Σ1278b background such that invasive growth assays could be performed.

The design of the phenotypic screen is outlined in Figure 1A and detailed in *Materials and Methods*. In brief, we drove gene overexpression by growth in galactose under conditions of nitrogen sufficiency; this approach identifies genes that upon overexpression can enable pseudohyphal growth in the absence of stimuli capable of inducing filamentation. To ensure that gene overexpression was efficient, we analyzed resulting protein levels by Western blotting for a sampling of seven strains in the constructed mutant collection (Figure S1). Filamentation was assessed by invasive growth analysis, as surface filamentation is lessened in the presence of galactose (Lorenz *et al.* 2000b). To confirm that invasive filamentation was indeed an effective indicator of diploid pseudohyphal growth, we cloned five genes along with native promoters into a high-copy yeast shuttle vector such that gene overexpression phenotypes could be measured without effects from galactose induction. Strains carrying the high-copy number vector clones yielded surface-spread filamentation phenotypes matching the corresponding invasive growth phenotypes observed in the screen (Figure S2). In addition, a positive control consisting of galactose-induced overexpression of eight genes known to affect pseudohyphal growth yielded exaggerated invasive phenotypes as shown in Figure 1B. The phenotypic difference between a wild-type strain and the indicated overexpression mutants is clear and establishes an easily identifiable threshold for positive results.

A collection of yeast genes capable of inducing pseudohyphal growth

By the systematic genome-wide overexpression analysis described above, we identified 551 genes that resulted in

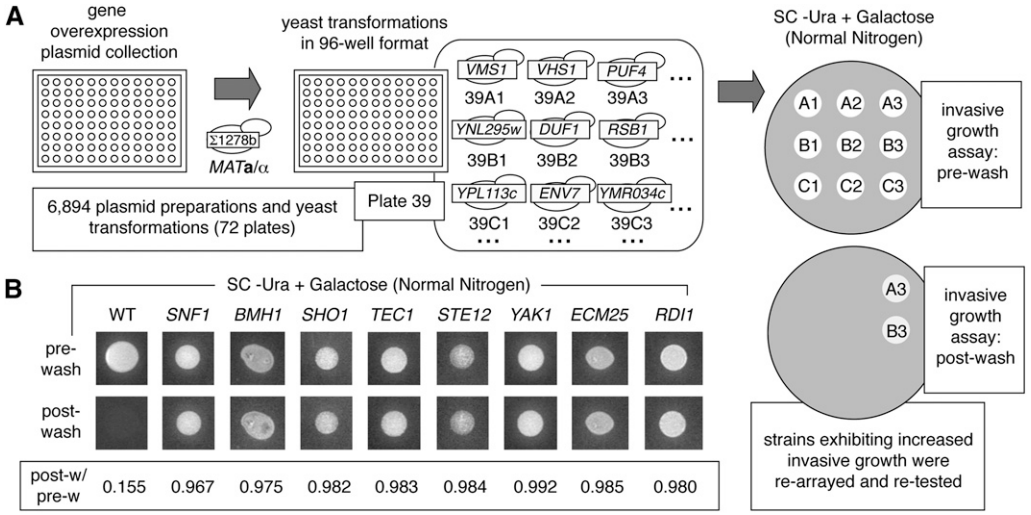

Figure 1 Systematic overexpression screen to identify genes capable of inducing filamentous growth. (A) Overview of the experimental design. Sample set of overexpression constructs from plate 39 (of 72 plates in total) is shown. Spotted cultures were assayed for invasive growth in an arrayed pattern with 48 spots per plate. Cultures were rearrayed in an altered pattern during retesting to control for positional effects. (B) Sampling of assay results for the wild-type background strain and eight overexpression mutants yielding invasive growth under conditions of nitrogen sufficiency. The degree of invasive growth was quantified by determining the pixel intensity of the spotted culture postwash relative to its prewash intensity. Complete listing of quantified scores for the genes identified in this screen is provided in Figure S3.

invasive filamentation upon galactose induction under conditions of nitrogen sufficiency (Figure 2A); the full gene list is provided in Figure S3. This gene set is comparable in size to the complement of genes that yield pseudohyphal growth defects upon gene deletion under conditions of butanol induction (Jin *et al.* 2008) and nitrogen deprivation (Ryan *et al.* 2012). The individual genes, however, vary between these gene sets, and the distinctions between overexpression-based screens *vs.* loss-of-function screens are presented in *Discussion*.

By simple Gene Ontology (GO) term analysis, the invasive growth overexpression gene set was not enriched for any molecular functions or protein-associated subcellular components; however, we did identify several enriched biological process terms (Figure 2B). Genes annotated as contributing to the regulation of metabolic processes associated with nitrogenous compounds were enriched in the overexpression gene set (*P*-value of 8.2×10^{-7}). This is not surprising since nitrogen availability is an important regulator of pseudohyphal growth. This GO term is broad in scope; among the associated genes are several known pseudohyphal growth regulators, including the *STE12* and *TEC1* genes that collectively encode a transcriptional complex acting downstream of Kss1p to activate gene promoters with filamentation-and-invasion response elements (FREs) (Madhani and Fink 1997). Genes involved in the cellular response to nutrient levels were also enriched in the results from our screen, as were overlapping gene sets associated with cytoskeletal organization and spindle pole body organization. The nutrient-responsive gene set encompasses the *SNF1* kinase gene, which plays an established role in regulating pseudohyphal growth (Kuchin *et al.* 2002). Interestingly, a large cohort of 79 functionally uncharacterized genes that lack a standard gene name indicative of function was identified in this screen. Mutant alleles of these genes lack extensive phenotypic characterization, and, for many of the indicated genes, the overexpression studies presented here offer initial insight into the regulatory consequences of increased transcription, particularly in a filamentous genetic background.

To consider the possibility that genes mediating specific cellular processes may affect pseudohyphal growth to differing degrees, we analyzed our quantified screening results for GO term enrichment within genes grouped by the intensity of observed overexpression-induced invasive growth (Figure 2D). The degree of invasive growth was estimated by the pixel intensity postwash to prewash of each spotted overexpression culture. The pixel intensities were binned into categories (ranging from 0.94 to 0.99 and above), and the associated genes within each grouping were assessed for enrichment of GO terms. By this analysis, genes annotated as being associated with M phase of the meiotic cell cycle (GO:0051327) were enriched in the gene set that yielded the strongest level of invasive growth upon overexpression (postwash:prewash pixel intensity greater than 0.99).

Signaling pathways that regulate pseudohyphal growth

While the GO term analysis above provides broad indications of cellular processes contributing to pseudohyphal growth, we also sought to identify specific pathways that affect filamentation by searching for KEGG signaling pathways overrepresented in the overexpression screen results. KEGG is an online database that provides annotated and manually drawn signaling pathway maps for a broad range of eukaryotes (www.genome.jp/kegg/). For our purposes, KEGG provides the largest set of yeast pathway annotations.

To identify enriched KEGG-annotated signaling pathways in our overexpression data set, we implemented a computational approach utilizing the functional annotation tool DAVID. By this analysis, we found pathways controlling cell cycle progression (sce04111), meiosis (sce04113), and MAPK signaling (sce04011) to be the most highly enriched in the overexpression data (Figure 3A). As these pathways encompass overlapping gene sets, we constructed network

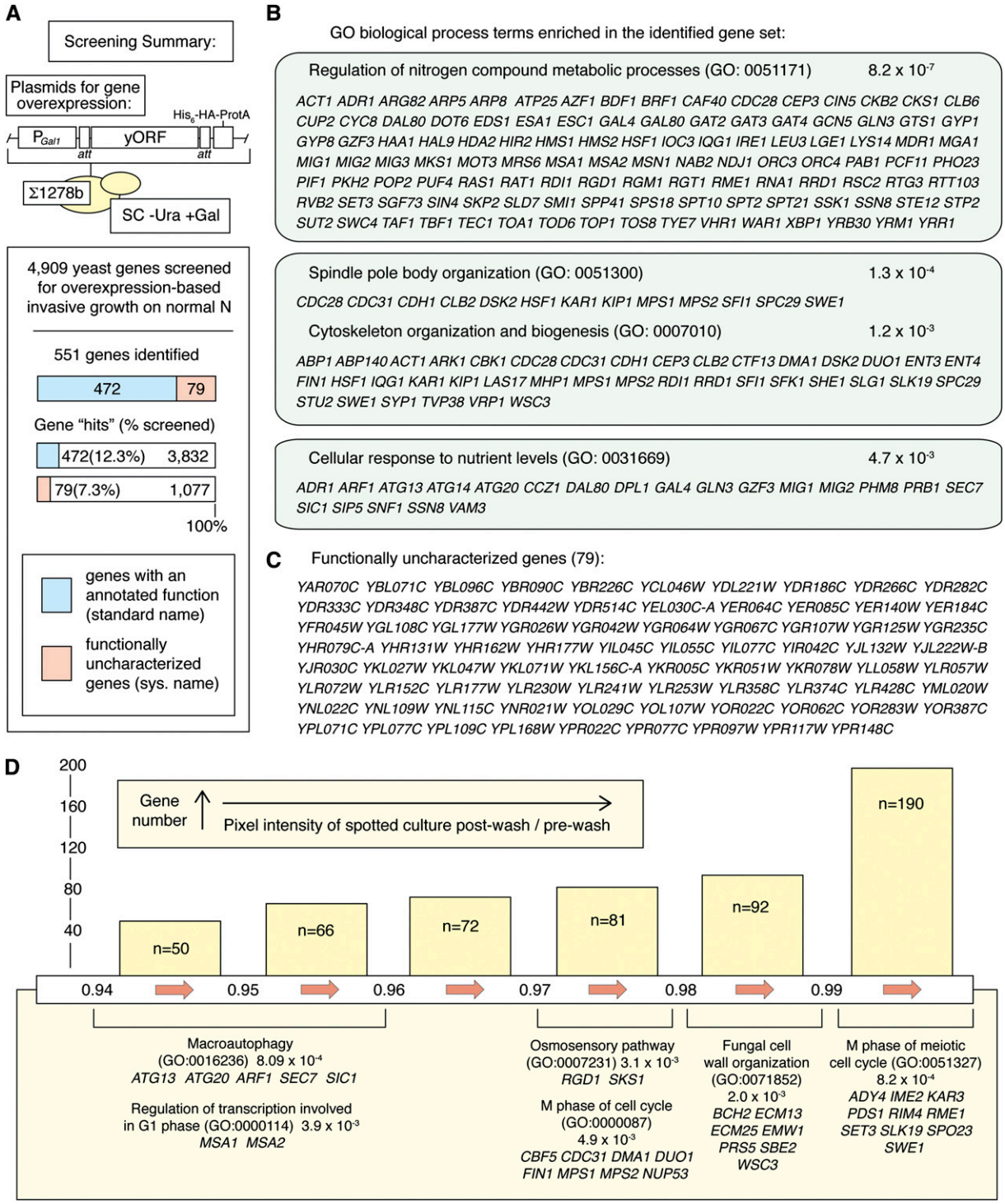

Figure 2 Summary of overexpression screen results. (A) Yeast genes were overexpressed by galactose induction using the indicated vector. Summary of screening results is presented below the vector diagram. The percentage of genes that yielded an overexpression-based filamentous growth phenotype is shown, with a breakdown separating functionally uncharacterized yeast genes from those with an annotated function and standard name. Percentages are indicated out of total genes screened per category. (B) Listing of Gene Ontology (GO) biological process categories enriched in the set of genes yielding filamentous growth phenotypes upon overexpression. Identified genes belonging to each category are indicated; extensively overlapping biological process categories are grouped together for convenience. (C) Listing of functionally uncharacterized genes identified in the screen. For purposes of this study, functionally uncharacterized genes are defined as such if they lack a standard gene name and lack GO biological process or molecular function annotation. (D) Quantified invasive growth scores were clustered and analyzed for enriched GO biological process terms. Identified GO terms are indicated along with gene "hits" annotated to each category. The number of genes (n) within each scoring range is indicated by the bar.

connectivity maps to better visualize the signaling modules (Figure 3B). Genes identified in the overexpression screen were used as core "seeds" along with other annotated components of the three pathways. The pathways were parsed using an in-house program and subsequently reassembled into a network using Cytoscape (*Materials and Methods*). Connections are visualized as ball-and-stick representations in Figure 3B. From this analysis, gene sets exhibiting genetic and/or physical interactions with components of the KEGG-annotated cell cycle and meiosis pathways were densely overlapping; this is not surprising since progression through the cell cycle and meiosis are obviously related processes. Genes exhibiting connections with MAPK signaling pathways share extensive connectivity with genes associated with meiosis and cell cycle progression. Interestingly, strictly from connections reported in the KEGG resources, the Kss1p and osmosensing Hog1p MAPK cascades link the MAPK signaling connectivity map with larger gene sets associated with cell cycle progression and meiosis (Figure 3B, inset).

Thus, from this analysis we identified core networks enriched in the data set mediating (1) MAPK signaling and (2) cell cycle progression/meiosis. Consequently, in the following sets of experiments we further investigated (1) the role of nuclear Hog1p in regulating pseudohyphal growth and (2) the genetic basis of pseudohyphal growth phenotypes resulting from altered cell cycle progression.

Hog1p-mediated repression of pseudohyphal growth

Genes annotated as contributing to MAPK signaling were enriched in the results of our overexpression screen; in particular, the screen identified several genes known to regulate the activity of Hog1p. The Hog1p kinase is a MAPK best studied for its role in producing glycerol as a compensatory osmolyte in response to increased levels of extracellular osmolarity (Kultz and Burg 1998; Westfall *et al.* 2008); however, Hog1p is also known to repress pseudohyphal growth in the absence of filamentation-inducing stimuli (O'Rourke and Herskowitz 1998; Pitoniak *et al.* 2009). A simplified representation of the Hog1p pathway is presented in Figure 4A. In yeast, high extracellular osmolarity stimulates two putative osmosensors, Sho1p and Sln1p (Posas and Saito 1997). Sho1p activates the P21-activated kinase family member Ste20p, which in turn activates a cascade of the MAPKKK Ste11p, the MAPKK Pbs2p, and Hog1p (Raitt *et al.* 2000). Sln1p, Ypd1p, and Ssk1p are components of a phosphorelay signaling system that activates the partially redundant kinases Ssk1p and Ssk22p upon osmostress; these kinases in turn activate Pbs2p, resulting in activation of Hog1p (Brewster *et al.* 1993; Maeda *et al.* 1994; Posas *et al.* 1996). Upon activation, Hog1p is rapidly translocated to the nucleus through a process that requires the importin-β family member Nmd5p (Ferrigno *et al.* 1998). Nuclear Hog1p has been identified in complexes at hundreds of promoters and genes, influencing chromatin remodeling and transcription (O'Rourke and Herskowitz 2004; Pokholok *et al.* 2006; Zapater *et al.* 2007). Subsequently, Hog1p is largely dephosphorylated by the phosphatases Ptc1p, Ptc2p, Ptc3p, Ptp2p, and Ptp3p (Robinson *et al.* 1994; Wurgler-Murphy *et al.* 1997; Mattison *et al.* 1999). Dephosphorylated Hog1p is exported into the cytosol through interaction with the karyopherin Crm1p (Ferrigno *et al.* 1998).

Interestingly, three genes involved in the nuclear export of Hog1p (*NBP2*, *PTP2*, and *CRM1*) were identified in the overexpression screen as enabling invasive growth under conditions of nitrogen sufficiency. To further consider the possibility that the nuclear export of Hog1p promotes pseudohyphal growth, we cloned the genes and promoters for *CRM1*, *NBP2*, *PTC3*, *PTP2*, and *PTP3* into a high-copy vector, enabling analysis of overexpression phenotypes without galactose induction. Each of these genes contributes to the dephosphorylation and nuclear export of Hog1p; *NBP2* is not illustrated in Figure 4A, but it recruits Ptc1p to the Pbs2p-Hog1p complex (Mapes and Ota 2004). We introduced these plasmids into a diploid strain of the filamentous Σ1278b genetic background and assayed for surface-spread filamentation under conditions of nitrogen limitation. In each case, the strains exhibited hyperactive surface filamentation relative to a wild-type strain carrying an empty vector control (Figure 4B).

Classically, the nuclear form of Hog1p had been thought to mediate osmotolerance; however, Westfall *et al.* (2008) reported that cells lacking *NMD5* and/or cells with a plasma membrane-tethered form of Hog1p survive hyperosmotic stress. This raises an interesting question regarding the functional contributions of nuclear Hog1p. Considering the overexpression results above, one function of nuclear Hog1p may be to repress pseudohyphal growth in a filamentation-competent strain of *S. cerevisiae*, although it should be noted that other pathways will also be affected by overexpression of genes such as *CRM1* and *NMD5*.

To investigate more directly the effect of spatial compartmentalization on Hog1p function, we constructed a haploid yeast strain in the Σ1278b background wherein endogenous *HOG1* was fused at its 3′ end to sequence encoding GFP and the nine C-terminal residues of Ras2p (designated CCAAX^{Ras2p}) as in Westfall *et al.* (2008). By virtue of S-palmitoylation and S-farnesylation of the cysteine residues in the appended Ras2p carboxy-terminal tail, the translated Hog1p-GFP-CCAAX^{Ras2p} chimera should localize at the plasma membrane, and we did observe concentrated fluorescence at the cell periphery in this strain (Figure 4C) relative to an otherwise isogenic strain containing an integrated *HOG1-GFP* allele. It should be noted that some Hog1p-GFP-CCAAX^{Ras2p} may be present at the nuclear membrane, although we did not observe any nuclear Hog1p chimera by fluorescence microscopy. Under pseudohyphal growth-inducing conditions of nitrogen stress and butanol treatment, the strain containing the Hog1p-GFP-CCAAX^{Ras2p} chimera showed slightly exaggerated invasive growth relative to a strain containing Hog1p-GFP, with invasive growth levels comparable to those observed in a *hog1*Δ strain. Under conditions of nitrogen sufficiency, the mutant strain

A

KEGG pathway	Identified genes
Cell cycle (sce04111)	*APC9, CDC28, CDH1, CKS1, CLB6, CYC8, FAR1, LTE1, MCM2, MPS1, ORC3, ORC4, PDS1, SIC1, SLK19, SWE1*
Meiosis (sce04113)	*APC9, CDC28, CLB6, IME2, MCM2, ORC3, ORC4, PDS1, RIM11, RME1, SIC1, SLK19, SNF1, SWE1, TPK3*
MAPK signaling pathway (sce04011)	*FAR1, GLO1, MSG5, SHO1, SLG1, SSK1, STE12, TEC1, WSC3*

B

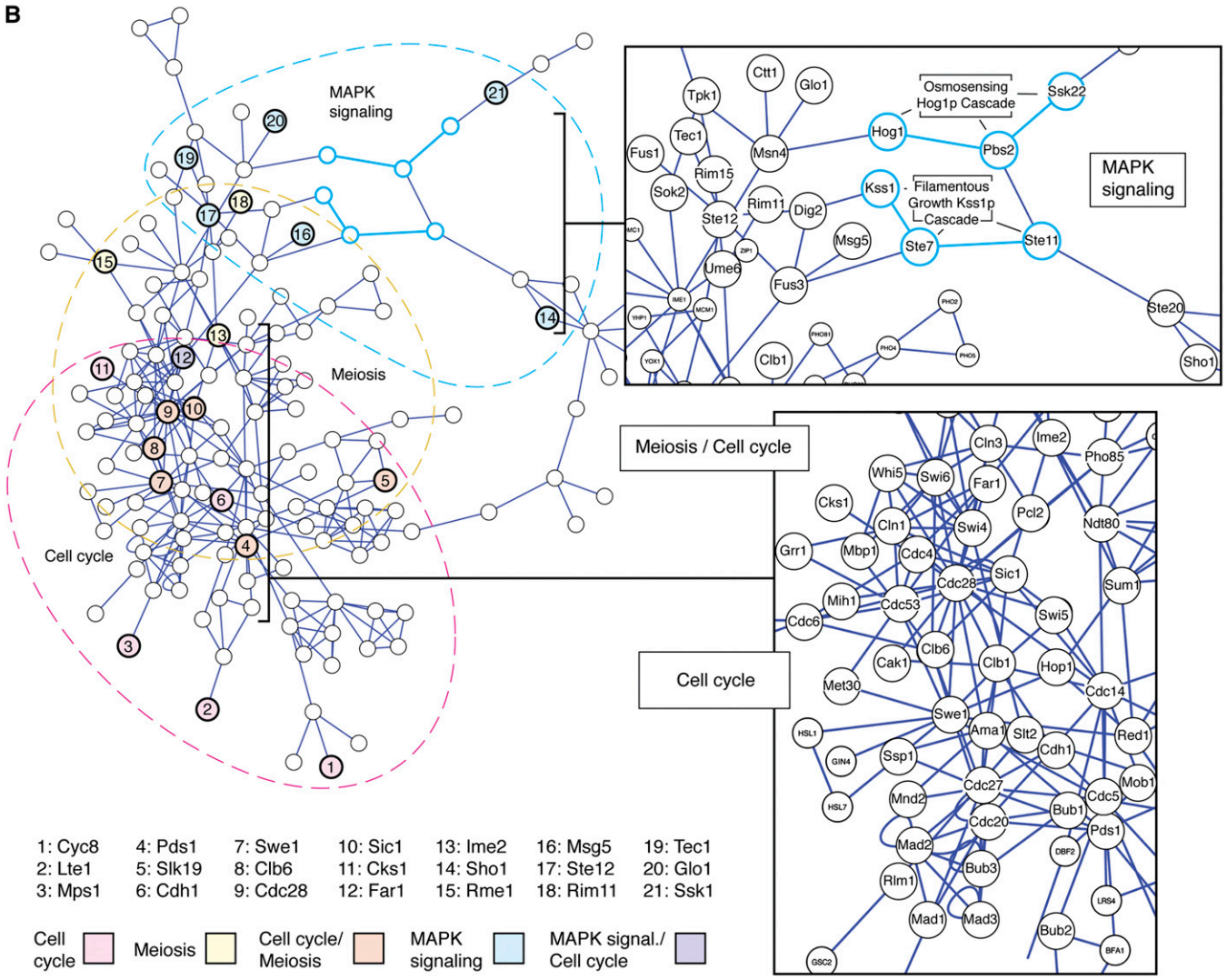

Figure 3 Identification of genetic networks that regulate the induction of filamentous growth. (A) The overexpression screen data set was analyzed for enrichment of pathways annotated in the Kyoto Encyclopedia of Genes and Genomes (KEGG). Enriched pathways are shown (cell cycle sce04111, meiosis sce04113, and MAPK signaling sce04011) along with genes identified in the screen that are annotated as belonging to the respective pathway. (B) Network connectivity map was built for the MAPK signaling, meiosis, and cell cycle networks from interactions annotated in KEGG. In-house programs were used to parse the pathway maps into nodes and edges for visualization using Cytoscape. The numbered circles indicate a subset of the genes identified in the overexpression screen that belong to the respective networks. Blowups of central portions of the cell cycle, meiosis, and MAPK signaling networks are provided, with key network components indicated in larger circles. Components of a given pathway in the map are indicated with a dashed line to highlight the overlap between networks. Two key connections between the MAPK signaling modules and the cell cycle/meiosis networks involving the Kss1p and Hog1p signaling cascades are shown in blue within the inset box.

containing Hog1p-GFP-CCAAX^{Ras2p} is hyperfilamentous with respect to a strain containing Hog1p-GFP, although not quite to the level of a *hog1*Δ strain; the degree of filamentous growth activity is measured in Figure 4C using a filamentation MAPK Kss1p pathway-specific FRE-*lacZ* reporter.

If nuclear Hog1p does repress pseudohyphal growth, filamentation should not be observed upon activation of the Hog1p pathway by high osmolarity. Under conditions of nitrogen stress and high salt, inducing both pseudohyphal growth and the Hog1p pathway, we find that a wild-type

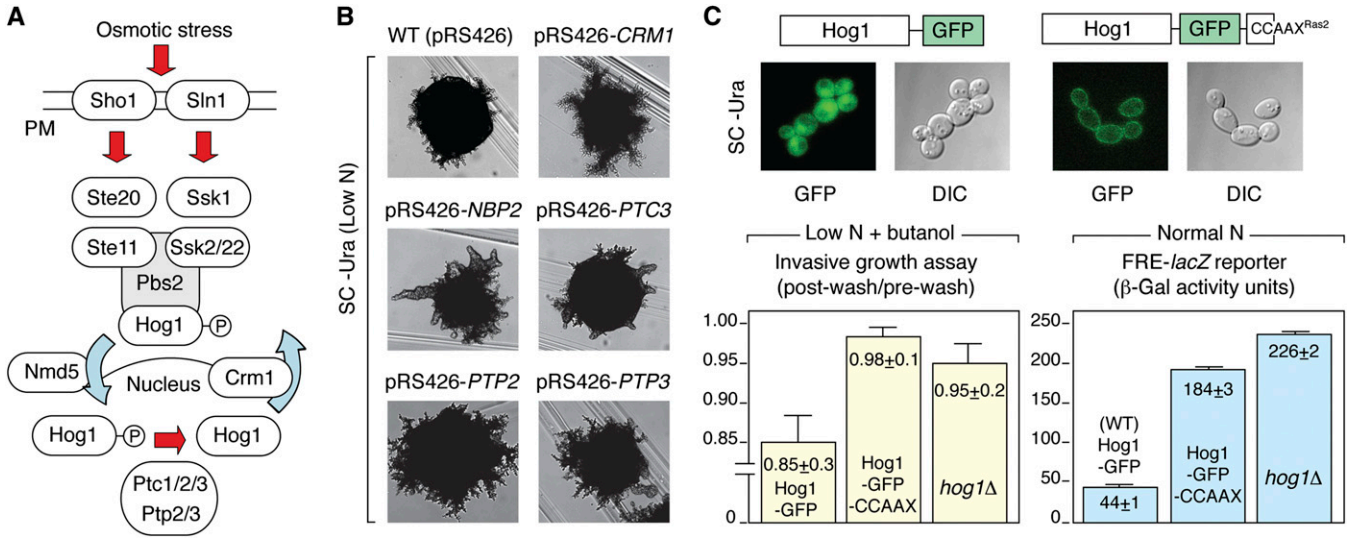

Figure 4 Regulated subcellular distribution of Hog1p and resulting filamentous growth phenotypes. (A) Diagram of the Hog1p MAPK osmosensing pathway. Regulated nuclear import and export of Hog1p is indicated. (B) Surface filamentation of genes along with native promoters cloned into a high-copy number yeast shuttle vector; the high-copy vector allows for gene overexpression without galactose induction. The selected genes regulate Hog1p phosphorylation/localization, thereby negatively regulating Hog1p function. Resulting surface filamentation phenotypes indicate that the overexpression of genes promoting Hog1p nuclear export yields exaggerated filamentous growth phenotypes under conditions of nitrogen stress. (C) Fluorescence images indicate that Hog1p-GFP with the carboxy-terminal Ras palmitoylation/farnesylation tag localizes to the cell periphery. Differential interference contrast (DIC) images are shown along with fluorescence images. Invasive growth assay results are shown for a haploid filamentous strain of the Σ1278b background containing Hog1p-GFP and the plasma membrane-tethered Hog1p-GFP-CCAAX form; a homozygous diploid strain in Σ1278b deleted for *HOG1* is also shown for purposes of comparison. The analysis was performed in triplicate, and mean values are shown. Error bars indicate standard deviation. Filamentous growth pathway activity was also assayed in the same three strains using a *lacZ* reporter driven from a promoter containing filamentation-responsive elements (FREs) recognized by the Ste12p/Tec1p transcription factor complex. Analyses were performed in triplicate, and mean results with standard deviation are indicated. Tethering Hog1p to the plasma membrane results in exaggerated invasive growth and hyperactivation of FRE-driven *lacZ* expression.

diploid strain of the filamentous Σ1278b background grows poorly and shows no signs of filament formation. Collectively, these findings are consistent with the notion that nuclear Hog1p contributes to the repression of pseudohyphal growth.

Genes contributing to exaggerated filamentous phenotypes from prolonged apical growth

Yeast cells undergo a switch from isotropic to apical growth upon progression through Start and a subsequent return to isotropic growth upon transition through G2/M (Hartwell *et al.* 1970; Lew and Reed 1993; Chant and Pringle 1995; Pringle *et al.* 1995). Genetic perturbations and/or chemical treatments that delay the G2/M transition in the filamentous Σ1278b strain result in a prolonged period of apical growth, as well as increased unipolar budding and decreased cell separation (Sheu *et al.* 2000; Miled *et al.* 2001; Rua *et al.* 2001). In yeast, the mitotic cyclins Clb1p and Clb2p antagonize polarized growth and are key in the molecular events underlying the onset of mitosis (Fitch *et al.* 1992; Booher *et al.* 1993), and a homozygous diploid *clb2*Δ/Δ strain is hyperfilamentous. Considering the importance of genes that regulate the apical–isotropic transition in affecting pseudohyphal growth phenotypes, we sought to determine if additional genes identified in our screen contributed to the hyperfilamentous phenotype of a *clb2*Δ mutant. We selected a sampling of 10 genes identified in our screen with unclear pathway designations and/or unclear roles in promoting pseudohyphal growth (*HMS1*, *HMS2*, *MGA1*, *MSB2*, *MSN1*, *NPR1*, *PTP3*, *SNF1*, *YAK1*, and *YCK1*) and generated homozygous diploid deletions of these genes in the *clb2*Δ/Δ background for phenotypic analysis; results are shown in Table 1 and Figure S4A. Notably, under conditions of nitrogen sufficiency, the majority of double mutants yielded phenotypes mirroring *clb2*Δ/Δ; however, the *clb2*Δ/Δ*msb2*Δ/Δ mutant exhibited a reduction in surface-spread filamentation relative to the *clb2*Δ/Δ parent. Increased apical growth resulting from hydroxyurea-induced cell cycle arrest in S phase has also been shown to drive surface-spread filamentation (Lorenz and Heitman 1998; Kang and Jiang 2005). Consequently, we also tested homozygous diploid single deletions of the same 10 genes indicated above for the absence of surface-spread filamentation upon hydroxyurea treatment. As indicated in Table 1 and Figure S4B, the *mga1*Δ/Δ, *msn1*Δ/Δ, *ptp3*Δ/Δ, and *msb2*Δ/Δ strains exhibited decreased surface filamentation in response to hydroxyurea treatment relative to the wild-type parent. From these results, the *msb2*Δ/Δ strain exhibited the most significant decrease in hydroxyurea-induced filamentation of the strains tested. Collectively, these studies highlight the contribution of Msb2p under genetic perturbations and chemical treatments that induce filamentation through prolonged apical growth.

Discussion

Here we implemented a systematic and genome-wide analysis of yeast invasive filamentation induced by gene overexpression. Interestingly, as compared against the results from large-scale deletion/disruption screens, systematic overexpression screens typically identify overlapping, but decidedly non-redundant, data sets (Sopko *et al.* 2006). We observe similar results here. In this screen, we identified 61 genes that were also reported in the targeted gene deletion screen by Ryan *et al.* (2012) and 79 genes that yielded pseudohyphal growth defects in a previous transposon-based disruption screen (Jin *et al.* 2008); a full listing of these overlapping genes is provided in Figure S5. Comparisons between these data sets are inexact, however, since: (1) filamentation phenotypes were assayed slightly differently in each screen; (2) the transposon-based study was smaller in scope, encompassing ~60% of the annotated yeast gene complement; (3) butanol treatment as opposed to nitrogen stress was used to induce filamentation in the transposon mutagenesis study; and (4) a haploid strain was used for transposon mutagenesis, while we used diploid cells for this overexpression screen. The partial overlap between loss-of-function and overexpression results likely stems from the fact that many genes can be required for a given cell process without being sufficient to induce that process upon overexpression. Consequently, we expected to identify a greater number of regulatory genes by this overexpression screen, and we did identify many such genes, including several that regulate cell cycle progression and MAPK signaling. However, we did not observe any statistically significant enrichment for transcription factors, kinases, and/or nutrient sensors in the data set, and the set of gene hits from this overexpression screen that overlapped the genes identified by targeted deletion and transposon-based loss-of-function screening was not significantly enriched for any GO terms. This overlapped gene set does encompass several key pseudohyphal growth genes, including *STE12*, *TEC1*, *SNF1*, and *SHO1*.

In interpreting the results from this study, it is important to bear in mind two caveats. First, 4909 genes (of 4973 verified ORFs) were analyzed by overexpression; thus, we do not consider the screen to be comprehensive, although it is the largest overexpression-based screen of pseudohyphal growth to date. Second, the plasmid library used in this study is a gene fusion library, and for a subset of the genes tested, the carboxy-terminal modification may result in dominant effects that can confound the interpretation of results. It is difficult to estimate the degree of this effect, but previous studies indicate that ~97% of the cloned gene products do encode full-length proteins (Gelperin *et al.* 2005), which may mitigate concerns regarding phenotypes from truncated proteins.

The gene set identified in this study appears large at first glance. However, systematic deletion studies in haploid and diploid strains of the Σ1278b background have identified comparably large sets of genes yielding pseudohyphal growth phenotypes. Our previous transposon-based disruption screen of 3627 genes identified 309 that were required for butanol-induced surface filamentation. Similarly, our previous smaller-scale overexpression screen identified 199 genes of 2043 tested that yielded exaggerated pseudohyphal growth under conditions of butanol induction (Jin *et al.* 2008). Extrapolating these results to the genome as a whole, we arrive again at comparably sized data sets. From these systematic disruption and overexpression screens, it is clear that many cellular processes need to occur effectively for surface filaments to appear. Cell cycle progression, cell budding, polarized growth, cytoskeletal organization, nutrient sensing/responses, and numerous metabolic/biosynthetic processes all contribute to, and are required for, the formation of extensive surface filaments. The pseudohyphal growth response represents an integrative output, the magnitude of which is modulated by a diverse complement of signaling pathways and genetic networks. In sum, the complexity and scope of the genetic machinery underlying yeast pseudohyphal growth makes it an ideal subject for genomic analysis.

Several genes that impacted the timing of G2/M progression in yeast were capable of inducing invasive growth upon overexpression. The results presented here are consistent with the importance of enhanced apical growth in establishing, at minimum, morphological phenotypes resembling those observed during pseudohyphal growth. We induced prolonged apical growth by genetic means (*clb2*Δ) and chemical treatment (hydroxyurea). Both sets of results highlight contributions from Msb2p, a mucin family member

Table 1 Filamentous phenotypes of mutants under prolonged apical growth

Strain	Growth medium	Surface filamentation phenotype
WT	SC medium	−
*clb2*Δ/Δ	SC medium	++
*clb2*Δ/Δ *hms1*Δ/Δ	SC medium	++
*clb2*Δ/Δ *hms2*Δ/Δ	SC medium	++
*clb2*Δ/Δ *mga1*Δ/Δ	SC medium	++
*clb2*Δ/Δ *msb2*Δ/Δ	SC medium	+
*clb2*Δ/Δ *msn1*Δ/Δ	SC medium	++
*clb2*Δ/Δ *npr1*Δ/Δ	SC medium	++
*clb2*Δ/Δ *ptp3*Δ/Δ	SC medium	++
*clb2*Δ/Δ *snf11*Δ/Δ	SC medium	++
*clb2*Δ/Δ *yak1*Δ/Δ	SC medium	++
*clb2*Δ/Δ *yck1*Δ/Δ	SC medium	++
WT	SC +hydroxyurea	++
*hms1*Δ/Δ	SC +hydroxyurea	++
*hms2*Δ/Δ	SC +hydroxyurea	++
*mga1*Δ/Δ	SC +hydroxyurea	+
*msb2*Δ/Δ	SC +hydroxyurea	−
*msn1*Δ/Δ	SC +hydroxyurea	+
*npr1*Δ/Δ	SC +hydroxyurea	++
*ptp3*Δ/Δ	SC +hydroxyurea	+
*snf1*Δ/Δ	SC +hydroxyurea	++
*yak1*Δ/Δ	SC +hydroxyurea	++
*yck1*Δ/Δ	SC +hydroxyurea	++

Surface filamentation: −, absence of filamentation; +, filamentation; ++, exaggerated filamentation.

that promotes activation of the MAPK Kss1p while also serving as an osmosensor for the HOG pathway; *msb2*Δ strains have been shown previously to exhibit decreased expression of a FRE-*lacZ* reporter and decreased filamentation (Cullen *et al.* 2004; Chavel *et al.* 2010). Interestingly, Msb2p was identified as a potential Cdc28p substrate through kinase assays using an analog-sensitive allele of Cdk1-Clb2p and lysate from a strain containing an Msb2p-GST fusion (Ubersax *et al.* 2003). With respect to the hydroxyurea-based results, Kang and Jiang (2005) previously screened the yeast deletion collection in a nonfilamentous genetic background for loss of what they termed to be semifilamentous growth induced by hydroxyurea treatment, identifying 16 genes that were required for the process. Each of those 16 genes was also required for hydroxyurea-induced filamentous growth in the filamentous Σ1278b background, and we found 4 of 10 genes independently selected in our study that yielded hydroxyurea-induced filamentation defects. Thus, a broader genome-wide screen in the Σ1278b background would likely reveal a large set of genes that contribute to this response, although some genetic networks required for nitrogen stress-induced pseudohyphal growth may not be required. It would further be interesting to determine if the filamentous response to hydroxyurea stems strictly from the S phase arrest or if genetic networks independent of cell cycle regulation also affect the observed filamentation.

MAPK signaling pathways are key pseudohyphal growth regulators, and the scope of genes identified in this screen that affect filamentation by impacting a MAPK signaling pathway may be large, as suggested from the network analysis presented here. In particular, our data encompass the known MAPK regulators/effectors *SHO1*, *MSB2*, *PTP3*, *STE12*, and *TEC1*, and 17 genes identified in this overexpression screen also exhibited increased mRNA transcript abundance upon induction of MAPK pathway activity (Roberts *et al.* 2000).

With respect to understanding MAPK cascade activity, considerable research efforts have been expended to consider the mechanisms ensuring MAPK signaling specificity during pseudohyphal growth (Bao *et al.* 2004; Maleri *et al.* 2004; O'Rourke and Herskowitz 2004; Hao *et al.* 2008). In particular, the Hog1p MAPK pathway is known to inhibit pseudohyphal growth in the absence of filamentous growth-inducing stimuli, and *HOG1* deletion mutants exhibit hyperactive surface filamentation under nutrient-rich conditions (O'Rourke and Herskowitz 1998). Interestingly, several genes that promote nuclear export of the osmoregulatory MAPK Hog1p, induced invasive growth upon overexpression. The nuclear-localized form of Hog1p is generally thought to mediate the hyperosmotic response and presumably also represses pseudohyphal growth. This notion, however, has been called into question, as Westfall *et al.* (2008) have reported that a yeast strain containing an allele of *hog1* encoding a plasma membrane-tethered form of the protein is still resistant to hyperosomotic stress. If nuclear-localized Hog1p is not required for resistance to hyperosmotic stress, the possibility exists that one function of nuclear Hog1p may be to represses pseudohyphal growth. As presented here, our overexpression screen results are consistent with this possibility, and results using a plasma membrane-tethered form of Hog1p are also consistent with this model. Identification of the nuclear targets of Hog1p that mediate a repressive effect remains a future goal. The transcription factor Tec1p is a strong candidate, as Shock *et al.* (2009) propose that Hog1p prevents Tec1p binding to DNA.

The importance of Hog1p signaling in regulating pseudohyphal growth is not limited to *S. cerevisiae*. In *C. albicans*, Hog1 is involved in oxidative stress responses, osmotic stress responses, and in cell wall biosynthesis, and functional Hog1 represses the yeast-to-hyphal transition (San Jose *et al.* 1996; Alonso-Monge *et al.* 1999, 2003; Enjalbert *et al.* 2006). Notably, mutants defective for Hog1p function display reduced virulence in mice and increased susceptibility to phagocytic cells (Gonzalez-Parraga *et al.* 2010; Cheetham *et al.* 2011). The Hog1 MAPK cascade in *C. albicans* encompasses the MAPKK Pbs2 and the MAPKKK Ssk2 (Cheetham *et al.* 2007), although additional upstream and downstream regulators have not been elucidated as extensively as in *S. cerevisiae*. As this *Candida* network becomes more clearly delineated, it will be interesting to determine if the emerging model of Hog1p-mediated regulation of filamentous growth in *S. cerevisiae* is borne out and even further, the degree to which corresponding filamentous growth regulatory networks in baker's yeast contribute to hyphal development and virulence in *C. albicans*.

In sum, we present here the first systematic overexpression screen for genes capable of inducing yeast pseudohyphal growth. Our results provide overexpression phenotypes for a large number of genes with uncharacterized function, and it is tempting to speculate that some of these genes may exhibit functions in the filamentous Σ1278b background but not in nonfilamentous strains. We further identified several signaling networks that modulate pseudohyphal growth levels upon overexpression-based perturbation, and collectively, the work presents a significantly enhanced foundation for the mapping of genetic relationships within the pseudohyphal growth regulatory network.

Acknowledgments

We thank Damian J. Krysan, Daniel J. Klionsky, William Stanaforth-Donahue, and Paul J. Cullen for reagents and/or helpful discussions regarding the manuscript. We thank Lois Weisman for the use of her fluorescence microscope. This work was supported by grants 1R01-A1098450-01A1 from the National Institutes of Health and 1-FY11-403 from the March of Dimes (to A.K.).

Literature Cited

Ahn, S. H., A. Acurio, and S. J. Kron, 1999 Regulation of G2/M progression by the STE mitogen-activated protein kinase pathway in budding yeast filamentous growth. Mol. Biol. Cell 10: 3301–3316.

Alonso-Monge, R., F. Navarro-Garcia, G. Molero, R. Diez-Orejas, M. Gustin *et al.*, 1999 Role of the mitogen-activated protein kinase Hog1p in morphogenesis and virulence of Candida albicans. J. Bacteriol. 181: 3058–3068.

Alonso-Monge, R., F. Navarro-Garcia, E. Roman, A. I. Negredo, B. Eisman *et al.*, 2003 The Hog1 mitogen-activated protein kinase is essential in the oxidative stress response and chlamydospore formation in Candida albicans. Eukaryot. Cell 2: 351–361.

Bao, M. Z., M. A. Schwartz, G. T. Cantin, J. R. Yates, and H. Madhani, 2004 Pheromone-dependent destruction of the tec1 transcription factor is required for MAP kinase signaling specificity in yeast. Cell 119: 991–1000.

Berman, J., and P. E. Sudbery, 2002 Candida albicans: a molecular revolution built on lessons from budding yeast. Nat. Rev. Genet. 3: 918–930.

Bharucha, N., J. Ma, C. J. Dobry, S. K. Lawson, Z. Yang *et al.*, 2008 Analysis of the yeast kinome reveals a network of regulated protein localization during filamentous growth. Mol. Biol. Cell 19: 2708–2717.

Booher, R. N., R. J. Deshaies, and M. W. Kirschner, 1993 Properties of Saccharomyces cerevisiae wee1 and its differential regulation of p34CDC28 in response to G1 and G2 cyclins. EMBO J. 12: 3417–3426.

Braun, B. R., and A. D. Johnson, 1997 Control of filament formation in Candida albicans by the transcriptional repressor TUP1. Science 277: 105–109.

Brewster, J. L., T. De Valoir, N. D. Dwyer, E. Winter, and M. C. Gustin, 1993 An osmosensing signal transduction pathway in yeast. Science 259: 1760–1763.

Chant, J., and J. R. Pringle, 1995 Patterns of bud-site selection in the yeast Saccharomyces cerevisiae. J. Cell Biol. 129: 751–765.

Chavel, C. A., H. M. Dionne, B. Birkaya, J. Joshi, and P. J. Cullen, 2010 Multiple signals converge on a differentiation MAPK pathway. PLoS Genet. 6: e1000883.

Cheetham, J., D. A. Smith, A. Da Silva Dantas, K. S. Doris, M. J. Patterson *et al.*, 2007 A single MAPKKK regulates the Hog1 MAPK pathway in the pathogenic fungus Candida albicans. Mol. Biol. Cell 18: 4603–4614.

Cheetham, J., D. M. Maccallum, K. S. Doris, A. Da Silva Dantas, S. Scorfield *et al.*, 2011 MAPKKK-independent regulation of the Hog1 stress-activated protein kinase in Candida albicans. J. Biol. Chem. 286: 42002–42016.

Coelho, P. S., A. Kumar, and M. Snyder, 2000 Genome-wide mutant collections: toolboxes for functional genomics. Curr. Opin. Microbiol. 3: 309–315.

Cook, J. G., L. Bardwell, S. J. Kron, and J. Thorner, 1996 Two novel targets of the MAP kinase Kss1 are negative regulators of invasive growth in the yeast Saccharomyces cerevisiae. Genes Dev. 10: 2831–2848.

Cook, J. G., L. Bardwell, and J. Thorner, 1997 Inhibitory and activating functions for MAPK Kss1 in the S. cerevisiae filamentous growth signalling pathway. Nature 390: 85–88.

Cullen, P. J., and G. F. Sprague, 2000 Glucose depletion causes haploid invasive growth in yeast. Proc. Natl. Acad. Sci. USA 97: 13461–13463.

Cullen, P. J., W. Sabbagh, E. Graham, M. M. Irick, E. K. Van Olden *et al.*, 2004 A signaling mucin at the head of the Cdc42- and MAPK-dependent filamentous growth pathway in yeast. Genes Dev. 18: 1695–1708.

Dickinson, J. R., 1996 'Fusel' alcohols induce hyphal-like extensions and pseudohyphal formation in yeasts. Microbiology 142 (Pt 6): 1391–1397.

Douglas, A. C., A. M. Smith, S. Sharifpoor, Z. Yan, T. Durbic *et al.*, 2012 Functional analysis with a barcoder yeast gene overexpression system. G3 2: 1279–1289.

Dowell, R. D., O. Ryan, A. Jansen, D. Cheung, S. Agarwala *et al.*, 2010 Genotype to phenotype: a complex problem. Science 328: 469.

Enjalbert, B., D. A. Smith, M. J. Cornell, I. Alam, S. Nicholls *et al.*, 2006 Role of the Hog1 stress-activated protein kinase in the global transcriptional response to stress in the fungal pathogen Candida albicans. Mol. Biol. Cell 17: 1018–1032.

Ferrigno, P., F. Posas, D. Koepp, H. Saito, and P. A. Silver, 1998 Regulated nucleo/cytoplasmic exchange of HOG1 MAPK requires the importin beta homologs NMD5 and XPO1. EMBO J. 19: 5606–5614.

Fitch, I., C. Dahmann, U. Surana, A. Amon, K. Nasmyth *et al.*, 1992 Characterization of four B-type cyclin genes of the budding yeast Saccharomyces cerevisiae. Mol. Biol. Cell 3: 805–818.

Gancedo, J. M., 2001 Control of pseudohyphae formation in Saccharomyces cerevisiae. FEMS Microbiol. Rev. 25: 107–123.

Gavin, A. C., M. Bosche, R. Krause, P. Grandi, M. Marzioch *et al.*, 2002 Functional organization of the yeast proteome by systematic analysis of protein complexes. Nature 415: 141–147.

Gelperin, D., M. A. White, M. L. Wilkinson, Y. Kon, L. A. Kung *et al.*, 2005 Biochemical and genetic analysis of the yeast proteome with a movable ORF collection. Genes Dev. 19: 2816–2826.

Ghaemmaghami, S., W. K. Huh, K. Bower, R. W. Howson, A. Belle *et al.*, 2003 Global analysis of protein expression in yeast. Nature 425: 737–741.

Gimeno, C. J., P. O. Ljungdahl, C. A. Styles, and G. R. Fink, 1992 Unipolar cell divisions in the yeast S. cerevisiae lead to filamentous growth: regulation by starvation and RAS. Cell 68: 1077–1090.

Gonzalez-Parraga, P., R. Alonso-Monge, J. Pla, and J. C. Arguelles, 2010 Adaptive tolerance to oxidative stress and the induction of antioxidant enzymatic activities in Candida albicans are independent of the Hog1 and Cap1-mediated pathways. FEMS Yeast Res. 10: 747–756.

Granek, J. A., and P. M. Magwene, 2010 Environmental and genetic determinants of colony morphology in yeast. PLoS Genet. 6: e1000823.

Grenson, M., 1966 Multiplicity of the amino acid permeases in Saccharomyces cerevisiae. II. Evidence for a specific lysine-transporting system. Biochim. Biophys. Acta 127: 339–346.

Gueldener, U., J. Heinisch, G. J. Koehler, D. Voss, and J. H. Hegemann, 2002 A second set of loxP marker cassettes for Cre-mediated multiple gene knockouts in budding yeast. Nucleic Acids Res. 30: e23.

Guo, B., C. A. Styles, Q. Feng, and G. Fink, 2000 A Saccharomyces gene family involved in invasive growth, cell-cell adhesion, and mating. Proc. Natl. Acad. Sci. USA 97: 12158–12163.

Hao, N., S. Nayak, M. Behar, R. H. Shanks, M. J. Nagiec *et al.*, 2008 Regulation of cell signaling dynamics by the protein kinase-scaffold Ste5. Mol. Cell 30: 649–656.

Hartwell, L. H., J. Culotti, and B. Reid, 1970 Genetic control of the cell-division cycle in yeast. I. Detection of mutants. Proc. Natl. Acad. Sci. USA 66: 352–359.

Ho, Y., A. Gruhler, A. Heilbut, G. D. Bader, L. Moore *et al.*, 2002 Systematic identification of protein complexes in Saccharomyces cerevisiae by mass spectrometry. Nature 415: 180–183.

Huang Da, W., B. T. Sherman, and R. A. Lempicki, 2009 Systematic and integrative analysis of large gene lists using DAVID bioinformatics resources. Nat. Protoc. 4: 44–57.

Huh, W. K., J. V. Falvo, L. C. Gerke, A. S. Carroll, R. W. Howson *et al.*, 2003 Global analysis of protein localization in budding yeast. Nature 425: 686–691.

Jayatilake, J. A., Y. H. Samaranayake, L. K. Cheung, and L. P. Samaranayake, 2006 Quantitative evaluation of tissue invasion by wild type, hyphal and SAP mutants of Candida albicans, and non-albicans Candida species in reconstituted human oral epithelium. J. Oral Pathol. Med. 35: 484–491.

Jin, R., C. J. Dobry, P. J. Mccown, and A. Kumar, 2008 Large-scale analysis of yeast filamentous growth by systematic gene disruption and overexpression. Mol. Biol. Cell 19: 284–296.

Kanehisa, M., S. Goto, Y. Sato, M. Furumichi, and M. Tanabe, 2012 KEGG for integration and interpretation of large-scale molecular data sets. Nucleic Acids Res. 40: D109–D114.

Kang, C. M., and Y. W. Jiang, 2005 Genome-wide survey of nonessential genes required for slowed DNA synthesis-induced filamentous growth in yeast. Yeast 22: 79–90.

Karunanithi, S., N. Vadaie, C. A. Chavel, B. Birkaya, J. Joshi *et al.*, 2010 Shedding of the mucin-like flocculin Flo11p reveals a new aspect of fungal adhesion regulation. Curr. Biol. 20: 1389–1395.

Killcoyne, S., G. W. Carter, J. Smith, and J. Boyle, 2009 Cytoscape: a community-based framework for network modeling. Methods Mol. Biol. 563: 219–239.

Kron, S. J., C. A. Styles, and G. R. Fink, 1994 Symmetric cell division in pseudohyphae of the yeast Saccharomyces cerevisiae. Mol. Biol. Cell 5: 1003–1022.

Kuchin, S., V. K. Vyas, and M. Carlson, 2002 Snf1 protein kinase and the repressors Nrg1 and Nrg2 regulate FLO11, haploid invasive growth, and diploid pseudohyphal differentiation. Mol. Cell. Biol. 22: 3994–4000.

Kultz, D., and M. Burg, 1998 Evolution of osmotic stress signaling via MAP kinase cascades. J. Exp. Biol. 201: 3015–3021.

Kumar, A., S. Desetages, P. Coelho, G. Roeder, and M. Snyder, 2000 High-throughput methods for the large-scale analysis of gene function by transposon tagging. Methods Enzymol. 328: 550–574.

Kumar, A., S. Agarwal, J. A. Heyman, S. Matson, M. Heidtman *et al.*, 2002a Subcellular localization of the yeast proteome. Genes Dev. 16: 707–719.

Kumar, A., S. Vidan, and M. Snyder, 2002b Insertional mutagenesis: transposon-insertion libraries as mutagens in yeast. Methods Enzymol. 350: 219–229.

Leberer, E., C. Wu, T. Leeuw, A. Fourest-Lieuvin, J. E. Segall *et al.*, 1997 Functional characterization of the Cdc42p binding domain of yeast Ste20p protein kinase. EMBO J. 16: 83–97.

Lew, D. J., and S. I. Reed, 1993 Morphogenesis in the yeast cell cycle: regulation by Cdc28 and cyclins. J. Cell Biol. 120: 1305–1320.

Li, W., and A. P. Mitchell, 1997 Proteolytic activation of Rim1p, a positive regulator of yeast sporulation and invasive growth. Genetics 145: 63–73.

Liu, H., C. A. Styles, and G. R. Fink, 1993 Elements of the yeast pheromone response pathway required for filamentous growth of diploids. Science 262: 1741–1744.

Lo, H. J., J. Kohler, B. Didomenico, D. Loebenberg, A. Cacciapuoti *et al.*, 1997 Nonfilamentous C. albicans mutants are avirulent. Cell 90: 939–949.

Lo, W. S., and A. M. Dranginis, 1998 The cell surface flocculin Flo11 is required for pseudohyphae formation and invasion by Saccharomyces cerevisiae. Mol. Biol. Cell 9: 161–171.

Longtine, M. S., A. Mckenzie Iii, D. J. Demarini, N. G. Shah, A. Wach *et al.*, 1998 Additional modules for versatile and economical PCR-based gene deletion and modification in Saccharomyces cerevisiae. Yeast 14: 953–961.

Lorenz, M. C., and J. Heitman, 1998 Regulators of pseudohyphal differentiation in Saccharomyces cerevisiae identified through multicopy suppressor analysis in ammonium permease mutant strains. Genetics 150: 1443–1457.

Lorenz, M. C., N. S. Cutler, and J. Heitman, 2000a Characterization of alcohol-induced filamentous growth in Saccharomyces cerevisiae. Mol. Biol. Cell 11: 183–199.

Lorenz, M. C., X. Pan, T. Harashima, M. E. Cardenas, Y. Xue *et al.*, 2000b The G protein-coupled receptor gpr1 is a nutrient sensor that regulates pseudohyphal differentiation in Saccharomyces cerevisiae. Genetics 154: 609–622.

Ma, J., R. Jin, C. J. Dobry, S. K. Lawson, and A. Kumar, 2007a Overexpression of autophagy-related genes inhibits yeast filamentous growth. Autophagy 3: 604–609.

Ma, J., R. Jin, X. Jia, C. J. Dobry, L. Wang *et al.*, 2007b An interrelationship between autophagy and filamentous growth in budding yeast. Genetics 177: 205–214.

Ma, J., C. J. Dobry, D. J. Krysan, and A. Kumar, 2008 Unconventional genomic architecture in the budding yeast saccharomyces cerevisiae masks the nested antisense gene NAG1. Eukaryot. Cell 7: 1289–1298.

Madhani, H. D., and G. R. Fink, 1997 Combinatorial control required for the specificity of yeast MAPK signaling. Science 275: 1314–1317.

Madhani, H. D., C. A. Styles, and G. R. Fink, 1997 MAP kinases with distinct inhibitory functions impart signaling specificity during yeast differentiation. Cell 91: 673–684.

Madhani, H. D., T. Galitski, E. S. Lander, and G. R. Fink, 1999 Effectors of a developmental mitogen-activated protein kinase cascade revealed by expression signatures of signaling mutants. Proc. Natl. Acad. Sci. USA 96: 12530–12535.

Maeda, T., S. M. Wurgler-Murphy, and H. Saito, 1994 A two-component system that regulates an osmosensing MAP kinase cascade in yeast. Nature 369: 242–245.

Maleri, S., Q. Ge, E. A. Hackett, Y. Wang, H. G. Dohlman *et al.*, 2004 Persistent activation by constitutive Ste7 promotes Kss1-mediated invasive growth but fails to support Fus3-dependent mating in yeast. Mol. Cell. Biol. 24: 9221–9238.

Mapes, J., and I. M. Ota, 2004 Nbp2 targets the Ptc1-type 2C Ser/Thr phosphatase to the HOG MAPK pathway. EMBO J. 23: 302–311.

Mattison, C. P., S. S. Spencer, K. A. Kresge, J. Lee, and I. M. Ota, 1999 Differential regulation of the cell wall integrity mitogen-activated protein kinase pathway in budding yeast by the protein tyrosine phosphatases Ptp2 and Ptp3. Mol. Cell. Biol. 19: 7651–7660.

Miled, C., C. Mann, and G. Faye, 2001 Xbp1-mediated repression of CLB gene expression contributes to the modifications of yeast cell morphology and cell cycle seen during nitrogen-limited growth. Mol. Cell. Biol. 21: 3714–3724.

Minato, T., J. Wang, K. Akasaka, T. Okada, N. Suzuki *et al.*, 1994 Quantitative analysis of mutually competitive binding of human Raf-1 and yeast adenylyl cyclase to Ras proteins. J. Biol. Chem. 269: 20845–20851.

Mosch, H. U., and G. R. Fink, 1997 Dissection of filamentous growth by transposon mutagenesis in Saccharomyces cerevisiae. Genetics 145: 671–684.

Mosch, H. U., R. L. Roberts, and G. R. Fink, 1996 Ras2 signals via the Cdc42/Ste20/mitogen-activated protein kinase module to induce filamentous growth in Saccharomyces cerevisiae. Proc. Natl. Acad. Sci. USA 93: 5352–5356.

O'Rourke, S. M., and I. Herskowitz, 1998 The Hog1 MAPK prevents cross talk between the HOG and pheromone response MAPK pathways in Saccharomyces cerevisiae. Genes Dev. 12: 2874–2886.

O'Rourke, S. M., and I. Herskowitz, 2004 Unique and redundant roles for HOG MAPK pathway components as revealed by whole-genome expression analysis. Mol. Biol. Cell 15: 532–542.

Pan, X., and J. Heitman, 1999 Cyclic AMP-dependent protein kinase regulates pseudohyphal differentiation in Saccharomyces cerevisiae. Mol. Cell. Biol. 19: 4874–4887.

Pan, X., and J. Heitman, 2002 Protein kinase A operates a molecular switch that governs yeast pseudohyphal differentiation. Mol. Cell. Biol. 22: 3981–3993.

Peter, M., A. M. Neiman, H. O. Park, M. V. Lohuizen, and I. Herskowitz, 1996 Functional analysis of the interaction between the small GTP binding protein Cdc42 and the Ste20 protein kinase in yeast. EMBO J. 15: 7046–7059.

Pitoniak, A., B. Birkaya, H. M. Dionne, N. Vadaie, and P. J. Cullen, 2009 The signaling mucins Msb2 and Hkr1 differentially regulate the filamentation mitogen-activated protein kinase pathway and contribute to a multimodal response. Mol. Biol. Cell 20: 3101–3114.

Pokholok, D. K., J. Zeitlinger, N. M. Hannett, D. B. Reynolds, and R. A. Young, 2006 Activated signal transduction kinases frequently occupy target genes. Science 313: 533–536.

Posas, F., and H. Saito, 1997 Osmotic activation of the HOG MAPK pathway via Ste11p MAPKKK: scaffold role of Pbs2p MAPKK. Science 276: 1702–1705.

Posas, F., S. M. Wurgler-Murphy, T. Maeda, E. A. Witten, T. C. Thai *et al.*, 1996 Yeast HOG1 MAP kinase cascade is regulated by a multistep phosphorelay mechanism in the SLN1–YPD1-SSK1 "two-component" osmosensor. Cell 86: 865–875.

Pringle, J. R., E. Bi, H. A. Harkins, J. E. Zahner, C. De Virgilio *et al.*, 1995 Establishment of cell polarity in yeast. Cold Spring Harb. Symp. Quant. Biol. 60: 729–744.

Raitt, D. C., F. Posas, and H. Saito, 2000 Yeast Cdc42 GTPase and Ste20 PAK-like kinase regulate Sho1-dependent activation of the Hog1 MAPK pathway. EMBO J. 19: 4623–4631.

Roberts, C. J., B. Nelson, M. J. Marton, R. Stoughton, M. R. Meyer *et al.*, 2000 Signaling and circuitry of multiple MAPK pathways revealed by a matrix of global gene expression profiles. Science 287: 873–880.

Roberts, R. L., and G. R. Fink, 1994 Elements of a single MAP kinase cascade in Saccharomyces cerevisiae mediate two developmental programs in the same cell type: mating and invasive growth. Genes Dev. 8: 2974–2985.

Robertson, L. S., and G. R. Fink, 1998 The three yeast A kinases have specific signaling functions in pseudohyphal growth. Proc. Natl. Acad. Sci. USA 95: 13783–13787.

Robinson, M. K., W. H. Van Zyl, E. M. Phizicky, and J. R. Broach, 1994 TPD1 of Saccharomyces cerevisiae encodes a protein phosphatase 2C-like activity implicated in tRNA splicing and cell separation. Mol. Cell. Biol. 14: 3634–3645.

Rua, D., B. T. Tobe, and S. J. Kron, 2001 Cell cycle control of yeast filamentous growth. Curr. Opin. Microbiol. 4: 720–727.

Rupp, S., E. Summers, H. J. Lo, H. Madhani, and G. Fink, 1999 MAP kinase and cAMP filamentation signaling pathways converge on the unusually large promoter of the yeast FLO11 gene. EMBO J. 18: 1257–1269.

Ryan, O., R. S. Shapiro, C. F. Kurat, D. Mayhew, A. Baryshnikova *et al.*, 2012 Global gene deletion analysis exploring yeast filamentous growth. Science 337: 1353–1356.

San Jose, C., R. A. Monge, R. Perez-Diaz, J. Pla, and C. Nombela, 1996 The mitogen-activated protein kinase homolog HOG1 gene controls glycerol accumulation in the pathogenic fungus Candida albicans. J. Bacteriol. 178: 5850–5852.

Sheu, Y. J., Y. Barral, and M. Snyder, 2000 Polarized growth controls cell shape and bipolar bud site selection in Saccharomyces cerevisiae. Mol. Cell. Biol. 20: 5235–5247.

Shock, T. R., J. Thompson, J. R. Yates, and H. D. Madhani, 2009 Hog1 mitogen-activated protein kinase (MAPK) interrupts signal transduction between the Kss1 MAPK and the Tec1 transcription factor to maintain pathway specificity. Eukaryot. Cell 8: 606–616.

Sikorski, R. S., and P. Hieter, 1989 A system of shuttle vectors and yeast host strains designed for efficient manipulation of DNA in Saccharomyces cerevisiae. Genetics 122: 19–27.

Sopko, R., D. Huang, N. Preston, G. Chua, B. Papp *et al.*, 2006 Mapping pathways and phenotypes by systematic gene overexpression. Mol. Cell 21: 319–330.

St John, T. P., and R. W. Davis, 1981 The organization and transcription of the galactose gene cluster of Saccharomyces. J. Mol. Biol. 152: 285–315.

Ubersax, J. A., E. L. Woodbury, P. N. Quang, M. Paraz, J. D. Blethrow *et al.*, 2003 Targets of the cyclin-dependent kinase Cdk1. Nature 425: 859–864.

Vyas, V. K., S. Kuchin, C. D. Berkey, and M. Carlson, 2003 Snf1 kinases with different beta-subunit isoforms play distinct roles in regulating haploid invasive growth. Mol. Cell. Biol. 23: 1341–1348.

Westfall, P. J., J. C. Patterson, R. E. Chen, and J. Thorner, 2008 Stress resistance and signal fidelity independent of nuclear MAPK function. Proc. Natl. Acad. Sci. USA 105: 12212–12217.

Wurgler-Murphy, S. M., T. Maeda, E. A. Witten, and H. Saito, 1997 Regulation of the Saccharomyces cerevisiae HOG1 mitogen-activated protein kinase by the PTP2 and PTP3 protein tyrosine phosphatases. Mol. Cell. Biol. 17: 1289–1297.

Xu, T., C. A. Shively, R. Jin, M. J. Eckwahl, C. J. Dobry *et al.*, 2010 A profile of differentially abundant proteins at the yeast cell periphery during pseudohyphal growth. J. Biol. Chem. 285: 15476–15488.

Zapater, M., M. Sohrmann, M. Peter, F. Posas, and E. De Nadal, 2007 Selective requirement for SAGA in Hog1-mediated gene expression depending on the severity of the external osmostress conditions. Mol. Cell. Biol. 27: 3900–3910.

Communicating editor: D. Voytas

GENETICS

Supporting Information
http://www.genetics.org/lookup/suppl/doi:10.1534/genetics.112.147876/-/DC1

Genetic Networks Inducing Invasive Growth in *Saccharomyces cerevisiae* Identified Through Systematic Genome-Wide Overexpression

Christian A. Shively, Matthew J. Eckwahl, Craig J. Dobry, Dattatreya Mellacheruvu, Alexey Nesvizhskii, and Anuj Kumar

DOI: 10.1534/genetics.112.147876

Table S1. Strains used in this study.

Strain	Genotype	Source
Y825	*MATa ura3-52 leu2Δ0*	M. Snyder (Stanford U., CA)
HLY337	*MATα ura3-52 trp1-1*	G. Fink (MIT, MA)
Y825/6	*MATa/α ura3-52 leu2Δ0*	M. Snyder (Stanford U., CA)
YAK99	*MATa/α ura3-52/ura3-52 leu2Δ0 trp1-1* (HLY337 + Y825)	This study
YAK100	*MATa clb2Δ::URA3 ura3-52 leu2Δ0*	This study
YAK101	*MATα clb2Δ::URA3 ura3-52 trp1-1*	This study
YAK102	*MATa/MATα clb2Δ::URA3/clb2Δ::URA3 ura3-52/ura3-52 leu2Δ0 trp1-1*	This study
YAK103	*MATa hms1Δ::G418 ura3-52 leu2Δ0*	This study
YAK104	*MATα hms1Δ::G418 ura3-52 trp1-1*	This study
YAK105	*MATa/MATα hms1Δ::G418/hms1Δ::G418 ura3-52/ura3-52 leu2Δ0 trp1-1*	This study
YAK106	*MATa hms2Δ::G418 ura3-52 leu2Δ0*	This study
YAK107	*MATα hms2Δ::G418 ura3-52 trp1-1*	This study
YAK108	*MATa/MATα hms2Δ::G418/hms2Δ::G418 ura3-52/ura3-52 leu2Δ0 trp1-1*	This study
YAK109	*MATa mga1Δ::G418 ura3-52 leu2Δ0*	This study
YAK110	*MATα mga1Δ::G418 ura3-52 trp1-1*	This study
YAK111	*MATa/MATα mga1Δ::G418/mga1Δ::G418 ura3-52/ura3-52 leu2Δ0 trp1-1*	This study
YAK112	*MATa msb2Δ::G418 ura3-52 leu2Δ0*	This study
YAK113	*MATα msb2Δ::G418 ura3-52 trp1-1*	This study
YAK114	*MATa/MATα msb2Δ::G418/msb2Δ::G418 ura3-52/ura3-52 leu2Δ0 trp1-1*	This study
YAK115	*MATa msn1Δ::G418 ura3-52 leu2Δ0*	This study
YAK116	*MATα msn1Δ::G418 ura3-52 trp1-1*	This study
YAK117	*MATa/MATα msn1Δ::G418/msn1Δ::G418 ura3-52/ura3-52 leu2Δ0 trp1-1*	This study
YAK118	*MATa npr1Δ::G418 ura3-52 leu2Δ0*	This study
YAK119	*MATα npr1Δ::G418 ura3-52 trp1-1*	This study
YAK120	*MATa/MATα npr1Δ::G418/npr1Δ::G418 ura3-52/ura3-52 leu2Δ0 trp1-1*	This study
YAK121	*MATa ptp3Δ::G418 ura3-52 leu2Δ0*	This study

YAK122	*MATα ptp3Δ::G418 ura3-52 trp1-1*	This study
YAK123	*MATa/MATα ptp3Δ::G418/ptp3Δ::G418 ura3-52/ura3-52 leu2Δ0 trp1-1*	This study
YAK124	*MATa snf1Δ::G418 ura3-52 leu2Δ0*	This study
YAK125	*MATα snf1Δ::G418 ura3-52 trp1-1*	This study
YAK126	*MATa/MATα snf1Δ::G418/snf1Δ::G418 ura3-52/ura3-52 leu2Δ0 trp1-1*	This study
YAK127	*MATa yak1Δ::G418 ura3-52 leu2Δ0*	This study
YAK128	*MATα yak1Δ::G418 ura3-52 trp1-1*	This study
YAK129	*MATa/MATα yak1Δ::G418/yak1Δ::G418 ura3-52/ura3-52 leu2Δ0 trp1-1*	This study
YAK130	*MATa yck1Δ::G418 ura3-52 leu2Δ0*	This study
YAK131	*MATα yck1Δ::G418 ura3-52 trp1-1*	This study
YAK132	*MATa/MATα yck1Δ::G418/yck1Δ::G418 ura3-52/ura3-52 leu2Δ0 trp1-1*	This study
YAK133	*MATa clb2Δ::URA3 hms1Δ::G418 ura3-52 leu2Δ0*	This study
YAK134	*MATα clb2Δ::URA3 hms1Δ::G418 ura3-52 trp1-1*	This study
YAK135	*MATa/MATα clb2Δ::URA3/clb2Δ::URA3 hms1Δ::G418/hms1Δ::G418 ura3-52/ura3-52 leu2Δ0 trp1-1*	This study
YAK136	*MATa clb2Δ::URA3 hms1Δ::G418 ura3-52 leu2Δ0*	This study
YAK137	*MATα clb2Δ::URA3 hms1Δ::G418 ura3-52 trp1-1*	This study
YAK138	*MATa/MATα clb2Δ::URA3/clb2Δ::URA3 hms1Δ::G418/hms1Δ::G418 ura3-52/ura3-52 leu2Δ0 trp1-1*	This study
YAK139	*MATa clb2Δ::URA3 hms2Δ::G418 ura3-52 leu2Δ0*	This study
YAK140	*MATα clb2Δ::URA3 hms2Δ::G418 ura3-52 trp1-1*	This study
YAK141	*MATa/MATα clb2Δ::URA3/clb2Δ::URA3 hms2Δ::G418/hms2Δ::G418 ura3-52/ura3-52 leu2Δ0 trp1-1*	This study
YAK142	*MATa clb2Δ::URA3 mga1Δ::G418 ura3-52 leu2Δ0*	This study
YAK143	*MATα clb2Δ::URA3 mga1Δ::G418 ura3-52 trp1-1*	This study
YAK144	*MATa/MATα clb2Δ::URA3/clb2Δ::URA3 mga1Δ::G418/mga1Δ::G418 ura3-52/ura3-52 leu2Δ0 trp1-1*	This study
YAK145	*MATa clb2Δ::URA3 msb2Δ::G418 ura3-52 leu2Δ0*	This study
YAK146	*MATα clb2Δ::URA3 msb2Δ::G418 ura3-52 trp1-1*	This study
YAK147	*MATa/MATα clb2Δ::URA3/clb2Δ::URA3*	This study

	msb2Δ::G418/msb2Δ::G418 ura3-52/ura3-52 leu2Δ0 trp1-1	
YAK148	*MATa clb2Δ::URA3 msn1Δ::G418 ura3-52 leu2Δ0*	This study
YAK149	*MATα clb2Δ::URA3 msn1Δ::G418 ura3-52 trp1-1*	This study
YAK150	*MATa/MATα clb2Δ::URA3/clb2Δ::URA3 msn1Δ::G418/msn1Δ::G418 ura3-52/ura3-52 leu2Δ0 trp1-1*	This study
YAK151	*MATa clb2Δ::URA3 npr1Δ::G418 ura3-52 leu2Δ0*	This study
YAK152	*MATα clb2Δ::URA3 npr1Δ::G418 ura3-52 trp1-1*	This study
YAK153	*MATa/MATα clb2Δ::URA3/clb2Δ::URA3 npr1Δ::G418/npr1Δ::G418 ura3-52/ura3-52 leu2Δ0 trp1-1*	This study
YAK154	*MATa clb2Δ::URA3 ptp3Δ::G418 ura3-52 leu2Δ0*	This study
YAK155	*MATα clb2Δ::URA3 ptp3Δ::G418 ura3-52 trp1-1*	This study
YAK156	*MATa/MATα clb2Δ::URA3/clb2Δ::URA3 ptp3Δ::G418/ptp3Δ::G418 ura3-52/ura3-52 leu2Δ0 trp1-1*	This study
YAK157	*MATa clb2Δ::URA3 snf1Δ::G418 ura3-52 leu2Δ0*	This study
YAK158	*MATα clb2Δ::URA3 snf1Δ::G418 ura3-52 trp1-1*	This study
YAK159	*MATa/MATα clb2Δ::URA3/clb2Δ::URA3 snf1Δ::G418/snf1Δ::G418 ura3-52/ura3-52 leu2Δ0 trp1-1*	This study
YAK160	*MATa clb2Δ::URA3 yak1Δ::G418 ura3-52 leu2Δ0*	This study
YAK161	*MATα clb2Δ::URA3 yak1Δ::G418 ura3-52 trp1-1*	This study
YAK162	*MATa/MATα clb2Δ::URA3/clb2Δ::URA3 yak1Δ::G418/yak1Δ::G418 ura3-52/ura3-52 leu2Δ0 trp1-1*	This study
YAK163	*MATa clb2Δ::URA3 yck1Δ::G418 ura3-52 leu2Δ0*	This study
YAK164	*MATα clb2Δ::URA3 yck1Δ::G418 ura3-52 trp1-1*	This study
YAK165	*MATa/MATα clb2Δ::URA3/clb2Δ::URA3 yck1Δ::G418/yck1Δ::G418 ura3-52/ura3-52 leu2Δ0 trp1-1*	This study
YAK166	*Y825/6 + pRS426 [~1kb 5' of translation start + CRM1 + ~300bp 3' of translation stop]*	This study
YAK167	*Y825/6 + pRS426 [~1kb 5' of translation start + NBP2 + ~300bp 3' of translation stop]*	This study
YAK168	*Y825/6 + pRS426 [~1kb 5' of translation start + PTC3 + ~300bp 3' of translation stop]*	This study
YAK169	*Y825/6 + pRS426 [~1kb 5' of translation start + PTP2 + ~300bp 3' of translation stop]*	This study

YAK170	*Y825/6 + pRS426 [~1kb 5' of translation start + PTP3 + ~300bp 3' of translation stop]*	This study
YAK171	*Y825/6 + pRS426 [~1kb 5' of translation start + KDX1 + ~300bp 3' of translation stop]*	This study
YAK172	*Y825/6 + pRS426 [~1kb 5' of translation start + BIT61 + ~300bp 3' of translation stop]*	This study
YAK173	*Y825/6 + pRS426 [~1kb 5' of translation start + SSN8 + ~300bp 3' of translation stop]*	This study
YAK174	*Y825/6 + pRS426*	This study
YAK175	*MATa HOG1 – GFP – G418*	This study
YAK176	*MATa hog1Δ::G418*	This study
YAK177	*MATa HOG1 – GFP- CCAAX^{RAS2} – G418*	This study

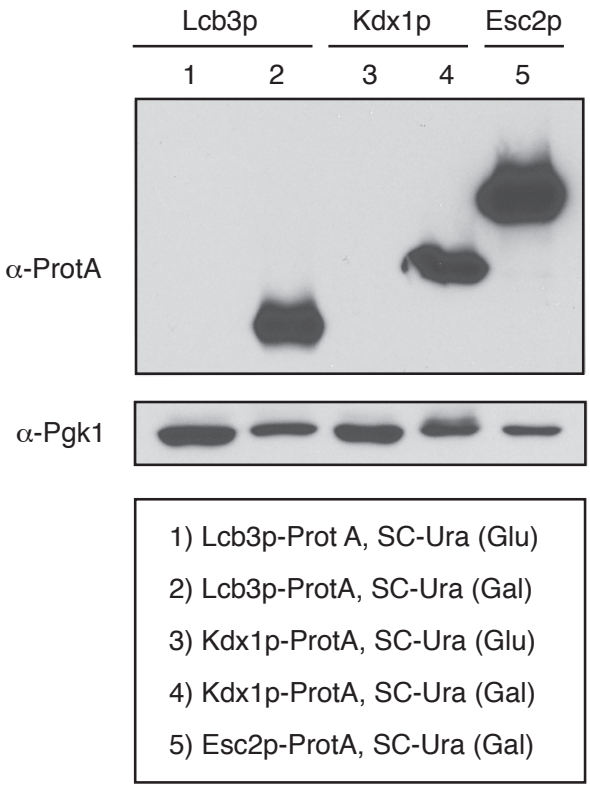

Figure S1 Western blot indicating galactose-induced overexpression of cloned genes. By virtue of the cloning vector, genes were fused at their 3'-ends to an affinity tag including sequence encoding the IgG binding domain from Protein A. Antibody against Protein A was used to detect the overexpressed gene product in medium with glucose and galactose, respectively. Pgk1p levels were assessed as a loading control. Seven overexpressed proteins in total were analyzed by Western blotting to confirm galactose induction (Apj1p, Erg9p, Esc1p, Esc2p, Kdx1p, Lcb3p, and Mgr1p); the expression of each gene product was strongly increased in galactose-containing medium, and results for Lcb3p, Kdx1p, and Esc2p are shown here.

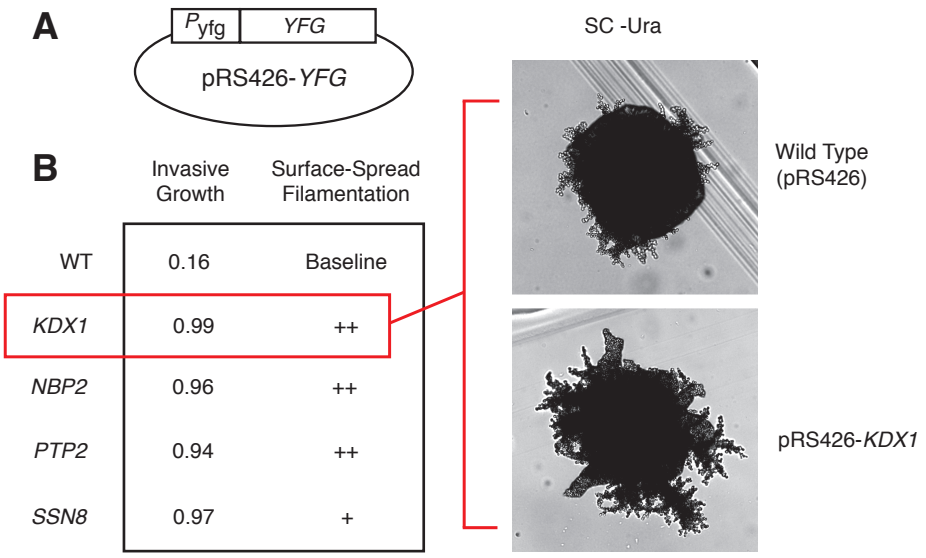

Figure S2 Gene overexpression phenotypes assessed without galactose induction. (A) Genes were cloned into the pRS426 yeast shuttle vector allowing for high copy levels in yeast; genes were cloned along with native promoters. *YFG*, Your Favorite Gene. (B) Invasive growth scores are shown along with qualitative surface filamentation phenotypes for a sampling of genes. Images (right column) are shown for a yeast strain of the filamentous Σ1278b background with the pRS426-*KDX1* construct; an isogenic strain carrying the empty pRS426 vector serves as a wild-type control. Surface filamentation was scored qualitatively, with the "++" and "+" designations indicating the extent of exaggerated filamentation.

Agar invasion score 0.94:

YAL024C, YAL027W, YBL079W, YBR276C, YCL046W, YCR005C, YDL051W, YDR186C, YDR289C, YDR348C, YGL006W, YGL057C, YGL110C, YGL123W, YGL227W, YGR240C, YHR002W, YIL078W, YKR005C, YKR035C, YKR077W, YLR102C, YLR152C, YLR399C, YLR451W, YML004C, YNL066W, YNL149C, YNL204C, YNL311C, YNR032W, YOL107W, YOL116W, YOR022C, YOR038C, YOR049C, YOR066W, YOR145C, YOR208W, YOR241W, YOR244W, YOR283W, YOR334W, YPL054W, YPL124W, YPL210C, YPL217C, YPR085C, YPR117W, YPR140W

Agar invasion score 0.95:

YAR031W, YBL063W, YBL091C-A, YBR021W, YBR152W, YBR226C, YDL113C, YDL192W, YDR034C, YDR162C, YDR170C, YDR295C, YDR514C, YEL005C, YER028C, YER140W, YGL122C, YGL167C, YGL177W, YGL226W, YGR028W, YGR043C, YGR107W, YGR112W, YHR036W, YHR085W, YHR162W, YIL104C, YIL153W, YIR042C, YJL192C, YJL222W-B, YKL051W, YKL135C, YKL156C-A, YKR051W, YLL004W, YLL006W, YLR079W, YLR259C, YLR328W, YLR358C, YLR409C, YLR428C, YMR098C, YMR102C, YMR193W, YMR205C, YNL055C, YNL318C, YOL104C, YOL165C, YOR062C, YOR109W, YOR236W, YOR344C, YOR387C, YPL022W, YPL207W, YPL235W, YPR054W, YPR079W, YPR113W, YPR119W, YPR148C, YPR185W

Agar invasion score 0.96:

YAL035W, YBL047C, YBL071C, YBR128C, YBR131W, YBR294W, YDL014W, YDL090C, YDL182W, YDR155C, YDR264C, YDR282C, YDR477W, YER144C, YER151C, YFL039C, YFL050C, YGL055W, YGL064C, YGL096W, YGL099W, YGR002C, YGR052W, YGR064W, YGR094W, YGR119C, YGR125W, YGR243W, YHR104W, YHR109W, YIL158W, YIR028W, YJL127C, YJL134W, YJR045C, YJR117W, YKL071W, YKL143W, YKL144C, YKL166C, YKR034W, YKR053C, YKR097W, YLL024C, YLR057W, YLR084C, YLR230W, YMR115W, YMR168C, YMR235C, YMR276W, YMR283C, YNL059C, YNL127W, YNL288W, YNR052C, YOR034C, YOR039W, YOR048C, YOR070C, YOR205C, YOR237W, YOR245C, YOR384W, YPL040C, YPL077C, YPL242C, YPR004C, YPR008W, YPR021C, YPR077C, YPR162C

Agar invasion score 0.97:

YAR007C, YBR024W, YBR260C, YDL028C, YDL089W, YDR085C, YDR130C, YDR173C, YDR212W, YDR266C, YDR333C, YDR376W, YDR387C, YDR464W, YDR517W, YEL030C-A, YEL040W, YER014W, YER025W, YER048C, YER165W, YER176W, YER177W, YFL055W, YFR050C, YGL049C, YGL061C, YGL075C, YGL108C, YGR042W, YGR131W, YGR172C, YGR175C, YGR229C, YGR248W, YGR252W, YHR006W, YHR007C, YHR024C, YHR115C, YIL015W, YIL101C, YIR001C, YIR027C, YJL042W, YJL132W, YJL157C, YJR095W, YJR125C, YKL084W, YKL172W, YKR069W, YLL023C, YLL038C, YLR006C, YLR008C, YLR175W, YLR258W, YML088W, YML130C, YMR003W, YMR006C, YMR063W, YMR153W, YNL025C, YNL135C, YNL175C, YNL189W, YNR021W, YOL029C, YOL054W, YOL100W, YOR060C, YOR090C, YOR168W, YOR172W, YOR188W, YOR194C, YOR257W, YPL168W, YPR022C

Agar invasion score 0.98:

YAR070C, YBL009W, YBL031W, YBL043W, YBL096C, YBL103C, YBR033W, YBR083W, YCL044C, YDL135C, YDL140C, YDR068W, YDR120C, YDR142C, YDR216W, YDR294C, YDR351W, YEL060C, YER037W, YER064C, YER088C, YER118C, YFL010C, YFR013W, YFR045W, YGL014W, YGL073W, YGL104C, YGL154C, YGL179C, YGL228W, YGR162W, YGR235C, YGR255C, YHR075C, YHR084W, YHR098C, YHR108W, YHR131W, YIL055C, YIR004W, YJL101C, YJL110C, YJL201W, YJR078W, YJR080C, YKL132C, YKL204W, YKR016W, YKR027W, YKR078W, YLL058W, YLR009W, YLR045C, YLR064W, YLR077W, YLR177W, YLR277C, YLR374C, YML020W, YML038C, YML051W, YMR101C, YMR139W, YMR140W, YMR241W, YMR302C, YNL022C, YNL064C, YNL077W, YNL097C, YNL115C, YNL169C, YNL255C, YNL299W, YNL313C, YNR067C, YOL006C, YOL061W, YOL105C, YOR065W, YOR197W, YOR324C, YOR335C, YOR356W, YOR370C, YPL109C, YPL160W, YPL246C, YPL248C, YPL270W, YPR173C

Agar invasion score >0.99:

YBL023C, YBL035C, YBL050W, YBL054W, YBL076C, YBR029C, YBR086C, YBR090C, YBR092C, YBR112C, YBR135W, YBR156C, YBR160W, YBR250W, YBR262C, YBR264C, YBR273C, YCL025C, YCL063W, YCR030C, YCR031C, YCR088W, YDL122W, YDL195W, YDL210W, YDL221W, YDL224C, YDR080W, YDR113C, YDR188W, YDR192C, YDR200C, YDR228C, YDR231C, YDR284C, YDR378C, YDR442W, YER032W, YER040W, YER085C, YER094C, YER105C, YER110C, YER114C, YER161C, YER184C, YFL027C, YFR023W, YGL003C, YGL023C, YGL035C, YGL066W, YGL164C, YGL166W, YGL180W, YGL181W, YGL209W, YGR026W, YGR044C, YGR067C, YGR096W, YGR100W, YGR105W, YGR109C, YGR123C, YGR159C, YGR218W, YGR246C, YGR249W, YGR274C, YHL024W, YHR014W, YHR032W, YHR079C, YHR135C, YHR161C, YHR177W, YIL045C, YIL056W, YIL077C, YIL094C, YIL136W, YIL137C, YIR013C, YJL047C, YJL054W, YJL090C, YJL092W, YJL105W, YJL106W, YJL141C, YJL187C, YJL191W, YJL200C, YJL204C, YJR030C, YJR093C, YJR116W, YJR147W, YKL027W, YKL038W, YKL047W, YKL119C, YKL129C, YKL146W, YKL161C, YKL210W, YKR002W, YKR029C, YKR088C, YLL003W, YLR013W, YLR072W, YLR136C, YLR227C, YLR241W, YLR251W, YLR253W, YLR273C, YLR337C, YLR357W, YLR403W, YLR405W, YML052W, YML057W, YML061C, YML076C, YML081W, YML086C, YMR010W, YMR032W, YMR070W, YMR094W, YMR136W, YMR179W, YMR182C, YMR212C, YMR219W, YMR309C, YNL020C, YNL053W, YNL076W, YNL109W, YNL161W, YNL182C, YNL183C, YNL188W, YNL233W, YNL236W, YNL238W, YNL251C, YNR034W, YNR059W, YOL013C, YOL089C, YOR008C, YOR028C, YOR032C, YOR098C, YOR101W, YOR106W, YOR113W, YOR118W, YOR138C, YOR141C, YOR162C, YOR181W, YOR195W, YOR227W, YOR239W, YOR251C, YOR271C, YOR299W, YOR307C, YOR317W, YOR360C, YPL055C, YPL071C, YPL105C, YPL125W, YPL128C, YPL158C, YPL222W, YPL250C, YPL269W, YPR009W, YPR026W, YPR097W, YPR141C, YPR157W

Figure S3 Listing of genes yielding invasion phenotypes upon gene overexpression. Agar invasion scores were generated as the pixel intensity of the spotted culture post-wash relative to its pre-wash intensity; genes are grouped according to these scores with the genes exhibiting strongest invasion yielding values of 0.99 or greater.

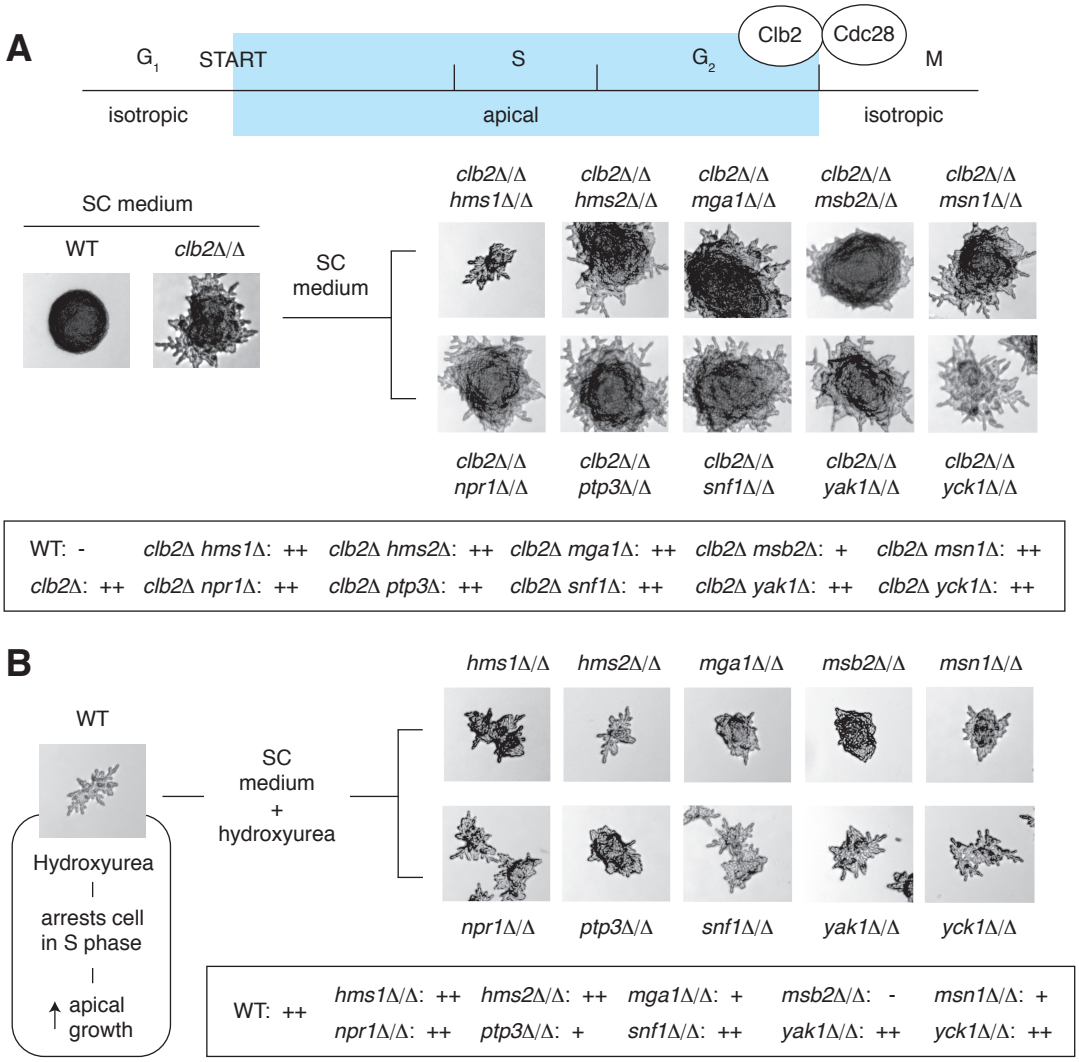

Figure S4 Analyzing the genetic basis of enhanced filamentous growth from perturbed cell cycle progression. (A) Surface-spread filamentation of indicated homozygous diploid *clb2*Δ double deletion mutants on standard growth medium under conditions of nitrogen sufficiency. The degree of observed filamentous growth is indicated in the boxed inset (as in Table 1). (B) filamentous growth induced by hydroxyurea treatment. Surface filamentation is shown for indicated homozygous diploid deletion mutants on standard growth medium supplemented with hydroxyurea. The degree of surface filamentation is qualitatively represented in the boxed inset as above.

A Genes exhibting filamentous growth phenotypes from both overexpression screening and gene deletion analysis: (61 genes)

YBL063W	*YDR289C*	*YGL003C*	*YGR255C*	*YLR337C*	*YNL076W*	*YOR066W*	*YPL055C*	*YPR119W*
YBR083W	*YDR387C*	*YGL014W*	*YHR084W*	*YLR357W*	*YNL097C*	*YOR205C*	*YPL109C*	*YPR140W*
YBR131W	*YDR477W*	*YGL064C*	*YJL092W*	*YML086C*	*YNL169C*	*YOR307C*	*YPL168W*	*YPR148C*
YCR088W	*YER014W*	*YGL228W*	*YJL101C*	*YMR063W*	*YNL175C*	*YOR317W*	*YPL222W*	*YPR157W*
YDL090C	*YER040W*	*YGR123C*	*YKL143W*	*YMR098C*	*YNL183C*	*YOR356W*	*YPL270W*	*YPR185W*
YDR120C	*YER118C*	*YGR162W*	*YKL204W*	*YMR193W*	*YNR034W*	*YPL022W*	*YPR026W*	
YDR162C	*YER161C*	*YGR229C*	*YLL006W*	*YNL053W*	*YOR065W*	*YPL040C*	*YPR097W*	

B Genes exhibting filamentous growth phenotypes from both overexpression screening and mTn-based gene disruption analysis: (79 genes)

YAR070C	*YDR282C*	*YER140W*	*YGR107W*	*YIL077C*	*YKR005C*	*YLR241W*	*YNR021W*	*YPL109C*
YBL071C	*YDR333C*	*YER184C*	*YGR125W*	*YIR042C*	*YKR051W*	*YLR253W*	*YOL029C*	*YPL168W*
YBL096C	*YDR348C*	*YFR045W*	*YGR235C*	*YJL132W*	*YKR078W*	*YLR358C*	*YOL107W*	*YPR022C*
YBR090C	*YDR387C*	*YGL108C*	*YHR079C-A*	*YJL222W-B*	*YLL058W*	*YLR374C*	*YOR022C*	*YPR077C*
YBR226C	*YDR442W*	*YGL177W*	*YHR131W*	*YJR030C*	*YLR057W*	*YLR428C*	*YOR062C*	*YPR097W*
YCL046W	*YDR514C*	*YGR026W*	*YHR162W*	*YKL027W*	*YLR072W*	*YML020W*	*YOR283W*	*YPR117W*
YDL221W	*YEL030C-A*	*YGR042W*	*YHR177W*	*YKL047W*	*YLR152C*	*YNL022C*	*YOR387C*	*YPR148C*
YDR186C	*YER064C*	*YGR064W*	*YIL045C*	*YKL071W*	*YLR177W*	*YNL109W*	*YPL071C*	
YDR266C	*YER085C*	*YGR067C*	*YIL055C*	*YKL156C-A*	*YLR230W*	*YNL115C*	*YPL077C*	

C Genes exhibiting filamentous growth phenotypes from current and previous (smaller) overexpression screens: (18 genes)

YBR083W	*YDR266C*	*YGL035C*	*YJR125C*	*YKL132C*	*YMR063W*	*YMR139W*	*YNL076W*	*YOR032C*
YCL044C	*YER040W*	*YGR240C*	*YKL051W*	*YML061C*	*YMR070W*	*YNL066W*	*YNL175C*	*YPL158C*

D Overexpression gene hits that also exhibited increased mRNA transcript levels upon activation of MAPK signaling: (17 genes)

YBL054W	*YBR226C*	*YDL135C*	*YEL060C*	*YGR123C*	*YJR078W*	*YKL161C*	*YOL104C*	*YPR141C*
YBR083W	*YBR294W*	*YDR085C*	*YGR043C*	*YJL157C*	*YJR095W*	*YNL053W*	*YPL054W*	

Figure S5 Overlap between genes showing filamentation phenotypes in the current overexpression study on medium with normal nitrogen levels and (A) systematic and targeted gene deletion analyses (invasive growth) under conditions of nutrient sufficiency; (B) large-scale transposon-based gene disruption analyses (surface filamentation) under conditions of butanol induction; C) previous overexpression analysis of 2043 constructs (surface filamentation) under conditions of butanol induction (Rin *et al., Mol. Biol. Cell*, 2008, 19:284) ; and D) increased mRNA abundance upon activation of MAPK signaling by various stimuli (Roberts *et al., Science*, 2000, 287: 873)